AD-A171 816   EXPANSION COEFFICIENT ON OXIDES AND OXIDE CERAMICS(U)   1/1
NAVAL WEAPONS CENTER CHINA LAKE CA J COVINO MAY 86
NWC-TP-6663 SBI-AD-E900 596
UNCLASSIFIED   F/G 11/2   NL

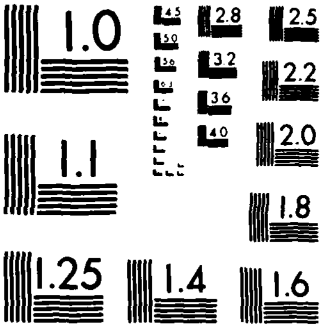

MICROCOPY RESOLUTION TEST CHART
NATIONAL BUREAU OF STANDARDS 1963 A

E900596

(12)

NWC TP 6663

Expansion Coefficient on Oxides and Oxide Ceramics

by
Josephine Covino
Research Department

MAY 1986

AD-A171 816

DTIC
S ELECTE D
AUG 1 5 1986
B

NAVAL WEAPONS CENTER
CHINA LAKE, CA 93555-6001

DTIC FILE COPY

Approved for public release; distribution is unlimited.

86 40

Naval Weapons Center

FOREWORD

Since the production of Cer-vit ceased, we have become increasingly dependent on Schott's Zerodur and Corning's ULE (type 7971) for use in applications requiring ultra-low thermal expansivity. There are times when neither ULE nor Zerodur are acceptable, particularly for laser gyros. In our search for a replacement for Cer-vit, we have begun by compiling the data found in the open literature through June 1985 on expansion coefficients of oxides and oxide ceramics. This report is the result of our gathering of this data.

This compilation was performed for Andrew Glista under NAVAIR Program Element 637-28-N, Project Number 137-831, Task Number W-1050, and Work Unit Number 137-831.

The report was reviewed for technical accuracy by Charlotte K. Lowe-Ma.

Approved by R. L. DERR, Head Research Department 15 May 1986	Under authority of K. A. DICKERSON Capt., USN Commander

Released for publication by
G. R. SCHIEFER
Technical Director

NWC Technical Publication 6663

Published by . . . . Technical Information Department
Collation . . . . Cover, 22 leaves
First printing . . . . 85 copies

UNCLASSIFIED
SECURITY CLASSIFICATION OF THIS PAGE

AD-A171 816

REPORT DOCUMENTATION PAGE

1a REPORT SECURITY CLASSIFICATION
UNCLASSIFIED

1b RESTRICTIVE MARKINGS

2a SECURITY CLASSIFICATION AUTHORITY

2b DECLASSIFICATION / DOWNGRADING SCHEDULE

3 DISTRIBUTION / AVAILABILITY OF REPORT
Approved for public release; distribution is unlimited.

4 PERFORMING ORGANIZATION REPORT NUMBER(S)
NWC TP 6663

5 MONITORING ORGANIZATION REPORT NUMBER(S)

6a NAME OF PERFORMING ORGANIZATION
Naval Weapons Center

6b OFFICE SYMBOL *(If applicable)*

7a NAME OF MONITORING ORGANIZATION

6c ADDRESS *(City, State, and ZIP Code)*
China Lake, CA 93555-6001

7b ADDRESS *(City, State, and ZIP Code)*

8a NAME OF FUNDING / SPONSORING ORGANIZATION
Naval Weapons Center

8b OFFICE SYMBOL *(If applicable)*

9 PROCUREMENT INSTRUMENT IDENTIFICATION NUMBER

8c ADDRESS *(City, State, and ZIP Code)*
China Lake, CA 93555-6001

10 SOURCE OF FUNDING NUMBERS

PROGRAM ELEMENT NO	PROJECT NO	TASK NO	WORK UNIT NO
637-28-N	137-831	W-1050	137-831

11 TITLE *(Include Security Classification)*
EXPANSION COEFFICIENTS ON OXIDES AND OXIDE CERAMICS

12 PERSONAL AUTHOR(S)
Josephine Covino

13a TYPE OF REPORT
Final

13b TIME COVERED
FROM 84 Dec TO 85 Jun

14 DATE OF REPORT *(Year, Month, Day)*
1986, May

15 PAGE COUNT
42

16 SUPPLEMENTARY NOTATION

17 COSATI CODES

FIELD	GROUP	SUB-GROUP
11	02	

18 SUBJECT TERMS *(Continue on reverse if necessary and identify by block number)*
Expansion Coefficients, Oxides, Structure Type, Unit Cell Parameters

19 ABSTRACT *(Continue on reverse if necessary and identify by block number)*

(U) Expansion coefficients for existing oxides and oxide ceramics have been compiled. In some cases, where data is available, a description of how the thermal expansion coefficient was measured will be noted.

20 DISTRIBUTION / AVAILABILITY OF ABSTRACT
☒ UNCLASSIFIED/UNLIMITED ☐ SAME AS RPT ☐ DTIC USERS

21 ABSTRACT SECURITY CLASSIFICATION
UNCLASSIFIED

22a NAME OF RESPONSIBLE INDIVIDUAL
Josephine Covino

22b TELEPHONE *(Include Area Code)*
619-939-1608

22c OFFICE SYMBOL
3854

DD FORM 1473, 84 MAR

83 APR edition may be used until exhausted
All other editions are obsolete

SECURITY CLASSIFICATION OF THIS PAGE
UNCLASSIFIED

CONTENTS

Figure:

Tables:

DTIC
ELECTE
AUG 15 1986
S D
B

DTIC
COPY
INSPECTED

Accession For
NTIS ✓
By
Dist
A-1

INTRODUCTION

Since the production of the glass ceramic Cer-vit ceased, we have become increasingly dependent on Schott's Zerodur and Corning's ULE (type 7971) for applications requiring ultra-low thermal expansivity; however, there are applications where neither ULE nor Zerodur are acceptable. For example, ULE has a high helium permeability and cannot be used for laser gyros. Zerodur cannot be used for all laser gyro applications because it is unstable on thermal cycling between -23 and 177°C (-9 and 350°F), which is the operational range of laser gyros. Furthermore, Zerodur is not of a reproducibly acceptable quality nor is it readily available. Because of these problems, the Navy needs new oxide glass ceramics with ultra-low expansion coefficients and low helium permeability.

This report is a compilation of data on expansion coefficients for existing oxides and oxide ceramics. Some of these materials may be suitable for laser gyro applications.

DISCUSSION

In the past 20 years, there has been an enormous growth of research effort in the measurement of thermal expansion coefficients of materials. These methods can be classified under the two general headings of microscopic (lattice) expansion measurements and macroscopic methods. The observations on thermal expansion can be made using either a static or a dynamic procedure. In the static procedure, the temperature of the material under investigation is maintained constant for a certain interval of time, and the variation of the length that takes place from one temperature to the other is measured.

The linear thermal expansion coefficient, α, at temperature T in kelvin units, can be calculated from the following empirical equation

$$\frac{3\alpha}{\chi_T} = \gamma \frac{C_v}{V} \tag{1}$$

where

χ_T = the isothermal compressibility of the solid
γ = the dimensionless quantity referred to has the Grüneisen constant (γ is about 2 and is temperature independent)
C_v = molar specific heat
V = volume of the solid, cm^3

At high temperatures, the empirical equation for a range of temperatures is given by

$$\alpha_T = A + B\,(T-T_0) + C\,(T-T_0)^2 \qquad (2)$$

while at very low temperatures

$$\alpha_T = Bt + DT^3 + ET^5 + \cdot \cdot \cdot \qquad (3)$$

where

A = the linear thermal expansion coefficient at temperature T_0 (K) and it is a factor expression in $10^{-6}/K$,
B = factor expressed $10^{-9}/K^2$
C = factor expressed $10^{-11}/K^3$
D = factor expressed $10^{-11}/K^4$
E = factor expressed $10^{-13}/K^6$, and
T = temperature in K

Equations 2 and 3 are purely empirical in that they have been derived from experimental results and observations. The numerical values of the quantities, A, B, C, etc., are given to two or three significant figures after the decimal point. The number of figures after the decimal point varies in Tables 1 and 2 because some materials have been studied more precisely than others. The columns entitled Method and Remarks give some indication of how α was measured. The details of the methods applied for measuring coefficients of thermal expansion reported in Tables 1 and 2 can be found in chapter 2 of R. S. Krishnan's book, Thermal Expansion of Crystals (Reference 1).

Table 1 presents a compilation of α_T for oxides at high temperatures and Table 2 presents some low-temperature data. Much of the description of structural variation with temperature depends on the use of thermal expansion coefficients of volume and linear structural units. Thus, it is important to recognize the limits in the accuracy of reported coefficients. Unit-cell expansion coefficients may be determined on single crystals or powders using either X-ray diffraction or dilatometry. Although the reported precision for many of those experiments is about 1% of the expansion coefficient, several studies on the same material commonly differ by ±10%.

TABLE 1. Thermal Expansion of Crystals Data (Reference 1).

Compound	Crystal systems	Axis	T_0, K	A	B	C	Range of temp, K[a]	Accuracy	Method	Remarks	Reference
Almandite $3FeO.Al_2O_3.3SiO_2$	Cubic	...	313	8.24	21.4	0.0	293-343	1[b]	I[c]	A garnet	2
Aluminum gallium arsenide $Al_{0.8}Ga_{0.2}As$	Cubic	...	...	3.1	...	...	163-363	15[d]	XR[e]	...	3
Aluminum tungstate $Al_4W_5O_{21}$	Cubic	...	...	1.9	...	...	298-973	...	XR	...	4
Ammonium aluminum alum $NH_4Al(SO_4)_2.12H_2O$	Cubic	...	...	6.65	...	...	at 273	1	I	...	5
Antimony oxide Sb_2O_3	Cubic	...	313	19.63	5.17	0.0	293-324	1	I	...	6
Arsenic oxide As_2O_3	Cubic	...	313	41.26	67.9	0.0	293-324	1	I	...	6
Barium nitrate $Ba(NO_3)_2$	Cubic	...	273	15.8	33.0	0.0	348-523	3	I	...	7
		...		17.0	0.0	0.0	195-288	1	P[f]	...	8
		...		6.7	0.0	0.0	78-195	1	P	...	8
		...		3.3	0.0	0.0	0-78	1	P	...	8
Barium titanate $BaTiO_3$	Cubic	a[g]	393	8.196	16.10	0.0	393-480		XR	Measurements made along tetragonal a-direction[h]	9
		a	623	7.482	9.727	0.0	623-1323		XR		10
Boracite $6MgO.MgCl_2.8B_2O_3$	Cubic	...	313	3.91	16.9	0.0	293-343	1	I	...	11
Cadmium ammonium sulphate $Cd_2(NH_4)_2(SO_4)_3$	Cubic	...	...	-11.4	...	...	at 300?	...	?	Ferroelectric T_c = 95 K[i]	12
Cobalt ferrite $CoFe_2O_4$	Cubic	...	273	7.326	15.16	0.080	300-938	...	XR	...	13
Cobalt tin ferrite $Co_{0.2}Sn_{0.8}Fe_2O_4$	Cubic	...	273	7.512	1.620	0.9340	300-938	...	XR	...	13

Data excerpted from Thermal Expansion of Crystals.

TABLE I. (Contd.)

Compound	Crystal systems	Axis	T_0, K	A	B	C	Range of temp, K^a	Accuracy	Method	Remarks	Reference
Grossularite $Ca_3Al_2(SiO_4)_3$	Cubic	...	313	6.93	17.0	0.0	293-343	1	I	A garnet	2
Lanthanum oxide La_2O_3	Cubic	...	273	4.94	16.1	-0.94	373-1323	...	QD^j	...^{k}	14
Magnesium oxide (Periclase) MgO	Cubic	... ...	273 273 200	10.98 11.01 9.43	5.865 5.23 12.60	0.1052 0.2001 -0.69	323-988 298-1151 300-1200	1 ... 1	I XR 3T-C^l	... ...^{k}	15 16 17
Magnesium oxide-tttrium oxide $MgO-Y_2O_3$	Cubic	...	...	12.5	...	...	at 473	...	...	...	18
Magnetite Fe_3O_4 $(Fe.Fe_2O_4)$	Cubic	...	273	8.417	4.051	4.146	314-843	1 ...	I ...	Curie point at 843 K	19
Manganous silicide MnSi	Cubic	...	...	-16.3	...	0.0	293-1073	...	...	Obeys a straight line variation	20
Nickel oxide NiO	Cubic	... ...	273	14.0 12.95	... 0.642	 0.069	at 1173 273-2273	... ...	XR XR	... ...^{k}	21 21
Sodium chlorate $NaClO_3$	Cubic	... ...	273	42.79 30.98	59.73 ...	7.201 ...	397-500 at 121.7	1 1	I I	... ...	22 23
Sodium tungstate $NaWO_4$	Cubic	...	273	17.68	27.66	0.0	293-873	...	I	...	24
Spessartite $3MnO.Al_2O_3.5SiO_2$	Cubic	...	313	8.24	21.4	0.0	293-343	1	I	A garnet	25
Spinel $MgAl_2O_4$ $(MgO.Al_2O_3)$	Cubic	...	313	5.93	19.5	0.0	293-343	1	I	...	26
Strontium titanate $SrTiO_3$	Cubic	... ...	273 ...	7.9 7.5	13.4 ...	0.4 ...	298-573 at 108	3 ...	I XR	Ferroelectric^l ...	27, 28 29

TABLE 1. (Contd.)

Compound	Crystal systems	Axis	T_0, K	A	B	C	Range of temp, K^a	Accuracy	Method	Remarks	Reference
Thorium oxide ThO_2	Cubic	...	1173	11.2	0.0	0.0	1173-2373	...	XR	CaF_2 type till 3473 K	30
Yttrium oxide Y_2O_3	Cubic	...	...	7.0	...	...	at 473	...		...	17
Zirconium tungstate ZrW_2O_3	Cubic	...	323	-10.3	0.0	0.0	323-475	...	XR	...	4
		...	473	-3.6	0.0	0.0	473-973	...	XR	...	4
Aluminum oxide (Alumina) Al_2O_3	Tri-gonal	c	273	6.582	4.995	0.2578	325-949	1	I	...	31
		a	273	5.425	5.534	0.2876	325-949	1	I	...	31
Aluminum oxide (Corundum) Al_2O_3	Tri-gonal	c	273	6.23	1.8	0.0	273-1173	...	QD	...	32
		a	273	5.85	2.05	0.0	273-1173	...	QD	...	32
Ammonium dihydrogen arsenate $NH_4H_2AsO_4$	Tetra-gonal	c	273	0.96	0.0	0.0	293-433	...	XR	Antiferroelectric	33
		a	273	17.52	55.02	0.0	293-433	...	XR	...	33
		c	223	5.8	0.0	0.0	223-323	...	I	...	34
		a	223	27.4	0.0	0.0	223-323	...	I	...	34
Ammonium dihydrogen phosphate $NH_4H_2PO_4$	Tetra-gonal	c	297	1.9	0.0	0.0	297-407	...	XR	Antiferroelectric	27
		a	297	39.3	0.0	0.0	297-407	...	XR	...	27
		c	223	4.2	0.0	0.0	223-323	...	I	...	34
		a	223	32.0	0.0	0.0	223-323	...	I	...	34
Ammonium iodide NH_4I	Tetra-gonal	c	273	64.67	494.2	0.0	97-231	...	XR	...^k	35
		a	273	1.935	-159.5	0.0	97-231	...	XR	...^k	35
Ammonium iodide (deuterated) ND_4I	Tetra-gonal	c	273	61.95	466.3	0.0	97-224	...	XR	...^h	35
		a	273	-12.72	-278.1	0.0	97-224	...	XR	...^h	35
Barium titanate $BaTiO_3$	Tetra-gonal	a	273	13.61	118.3	0.0	288-358	...	XR	Ferroelectric^h	9
		c	273	-0.158	-328.2	0.0	288-358	...	XR	T_c = 393 K^i	9
Barium tungstate $BaWO_4$	Tetra-gonal	c	273	17.45	28.797	3.0841	300-628	...	XR	...	36
		a	273	4.22	6.755	0.2965	300-628	...	XR	...	36

TABLE 1. (Contd.)

Compound	Crystal systems	Axis	T_0, K	A	B	C	Range of temp, K^a	Accuracy	Method	Remarks	Reference
Beryl (also emerald) $Al_2Be_3(SiO_3)_6$	Hexagonal	c	...	-2.9	...	...	at 300	...	XR	pure beryl	37
		a	...	2.6	...	...	at 300	...	XR	pure beryl	37
		c	313	-1.348	4.12	0.0	293-343	1	I	pure beryl	26
		a	313	1.0025	4.57	0.0	293-343	1	I	pure beryl	26
		c	...	0.16	...	...	at 300	...	XR	Cr-doped, i.e., emerald	37
		a	...	1.7	...	...	at 300	...	XR	Cr-doped, i.e., emerald	37
Beryllium oxide (bromallite) BeO	Hexagonal	c	273	5.82	5.8	0.0	300-1970	...	XR	...^{h}	38
		a	273	6.91	6.0	0.0	300-1970	...	XR	...^{h}	38
Beryllium silicate (phenacite) Be_2SiO_4	Trigonal	c	313	3.79	21.3	0.0	293-343	1	I	...	11
		a	313	2.99	23.0	0.0	293-343	1	I	...	11
Bismuth ferrite $BiFeO_3$	Hexagonal	c	298	15.1	0.0	0.0	298-598	...	XR	Ferroelectric	39
		a	298	10.9	0.0	0.0	298-598	...	XR	T = 1120 K	39
		c	(617?)	65.0	-180.0	20.3	217-1111	...	XR	D = -10 x 3	39
		a	617	12.2	0.0	0.0	617-1111	...	XR	x 10^{-14}	39
Brucite $Mg(OH)_2$	Trigonal	c	293	44.7	0.0	0.0	293-373	4.5$^+$	XR	...	40, 41
		a	293	11.0	0.0	0.0	293-373	13.5$^+$	XR	...	40, 41
Cadmium molybdate $CdMoO_4$	Tetragonal	c	273	14.91	7.00	1.098	301-353	...	XR	...	42
		a	273	6.10	25.43	-1.915	301-353	...	XR	...	42
Calcite $CaCO_3$	Trigonal	c	273	24.67	17.42	-0.5141	301-797	3	XR	...	43
		a	273	-3.660	-0.7112	-0.3339	301-797	3	XR	...	43
		c	273	24.71	37.75	-3.653	348-673	3	I	...	44
		c	273	24.39	5.33	-30.7	123-273	1	I	...	45
		a	273	-5.68	0.333	-4.58	123-373	3	I	...	45
Calcium hydroxide $Ca(OH)_2$	Hexagonal	c	293	33.4	0.0	0.0	293-373	6$^+$	XR	...	40, 41
		a	293	9.8	0.0	0.0	293-373	8$^+$	XR	...	40, 41
Calcium magnesium carbonate (Dolomite) $(Ca,Mg)CO_3$	Trigonal	c	313	20.6	36.8	0.0	293-343	1	I	...	46
		a	313	4.15	19.3	0.0	293-343	1	I	...	46

TABLE 1. (Contd.)

Compound	Crystal systems	Axis	T_0, K	A	B	C	Range of temp, K[a]	Accuracy	Method	Remarks	Reference
Calcium molybdate (powellite) $CaMoO_4$	Tetragonal	c	273	11.17	22.99	1.614	303-628	...	XR	...	47
		a	273	7.20	15.96	-0.154	303-628	...	XR	...	47
Calcium tungstate (scheelite) $CaWO_4$	Tetragonal	c	273	11.69	22.07	2.143	303-623	...	XR	...	48
		a	273	5.96	12.23	2.485	303-623	...	XR	...	48
Cassiterite SnO_2	Tetragonal	c		3.7	...		at 298	...	XR	...	49
		c	313	3.9	12.0	0.0	293-343	1	I	...	50
		a	313	3.2	7.6	0.0	293-343	1	I	...	50
Cerium oxide CeO_2	Tetragonal		273	64.17	1.572	0.0	304-1300	...	XR	...[h]	51
Cerium magnesium nitrate $Ce_2Mg_3(NO_3)_{12}.24H_2O$	Trigonal	c	...	-0.7	...	...	at 10	...	...	...	52
		c	...	3.7	...	...	at 20	...	...	...	52
		c	...	9.5	...	...	at 30	...	...	...	52
		c	...	20.4	...	...	at 50	...	...	...	52
		c	...	43.9	...	...	at 100	...	...	...	52
		c	...	72.2	...	...	at 200	...	...	...	52
		c	...	99.0	...	...	at 300	...	...	...	52
		a	...	0.1	...	...	at 10	...	...	...	52
		a	...	1.0	...	...	at 20	...	...	...	52
		a	...	2.6	...	...	at 30	...	...	...	52
		a	...	6.8	...	...	at 50	...	...	...	52
		a	...	12.6	...	...	at 100	...	...	...	52
		a	...	14.3	...	...	at 200	...	...	...	52
		a	...	14.7	...	...	at 300	...	...	...	52
Chromium dioxide CrO_2		c	...	-15.0	...	...	at 298	...	XR	...	53
		a		18.7	...	...	at 298	...	XR	...	53
		c		-0.1	...	...	at 643	...	XR	...	53
		a		13.5	...	...	at 643	...	XR	...	53
Gallium sesquioxide (α) Ga_2O_3	Trigonal	c	273	9.347	6.591	-0.011321	303-873	...	...	...	54
		a	273	5.232	8.651	-0.010419	303-875	...	...	...	54
Germanium dioxide GeO_2		c		1.7	...	...	at 298	...	XR	...	53
		a		6.1	...	...	at 298	...	XR	...	53
		c		5.6	...	...	at 923	...	XR	...	53
		a		11.6	...	...	at 923	...	XR	...	53

TABLE 1. (Contd.)

Compound	Crystal systems	Axis	T_0, K	A	B	C	Range of temp, K[a]	Accuracy	Method	Remarks	Reference
Guanadine aluminum sulphate hexahydrate (GASH) $C(NH_2)_3Al(H_2O)_6(SO_4)_2$	Hexagonal	c	298	93.3	0.0	0.0	298-328	...	XR	Ferroelectric no T_c	55
		a	298	10.0	0.0	0.0	298-328	...	XR		55
Haematite Fe_2O_3	Trigonal	c	273	9.34	1.644	0.0	273-1270	...	XR	...	56
		a	273	10.54	4.452	0.0	273-1270	...	XR	...	56
		c	273	7.897	5.285	7.318	320-670	1	I	...	57
		a	273	7.834	10.47	11.72	320-670	1	I	...	57
Lanthanum magnesium nitrate $La_2Mg_3(NO_3)_{12}\cdot 24H_2O$	Trigonal	c	...	-0.7	...	...	at 10	...	...		
		c	...	3.2	...	...	at 20	...	...	...	52
		c	...	8.5	...	...	at 30	...	...	...	52
		c	...	20.4	...	...	at 50	...	...	...	52
		c	...	43.8	...	...	at 100	...	...	...	52
		c	...	72.2	...	...	at 200	...	...	...	52
		c	...	99.0	...	...	at 300	...	...	...	52
		a	...	0.1	...	...	at 10	...	...	...	52
		a	...	1.0	...	...	at 20	...	...	...	52
		a	...	2.6	...	...	at 30	...	...	...	52
		a	...	6.8	...	...	at 50	...	...	...	52
		a	...	12.6	...	...	at 100	...	...	...	52
		a	...	14.3	...	...	at 200	...	...	...	52
		a	...	14.7	...	...	at 300	...	...	...	52
Lead dioxide PbO_2	Tetragonal	c	...	9.3	...	...	at 298	...	XR	...	53
		a	...	8.4	...	...	at 298	...	XR	...	53
Lead molybdate (wulfenite) $PbMoO_4$	Tetragonal	c	273	19.24	38.67	-4.805	301-628	...	XR	...	58
		a	273	8.14	19.38	0.823	301-628	...	XR	...	58
Lead tungstate (stolzite) $PbWO_4$	Tetragonal	c	273	19.59	3.77	2.888	301-628	...	XR	...	59
		a	273	8.12	0.4647	0.0	301-628	...	XR	...	59
Lithium aluminum ortho-silicate $LiAlSiO_4$ (β-eucryptite)	Hexagonal	c	300	-15.2	0.0	0.0	293-1373	...	XR	...	60
		a	300	7.9	0.0	0.0	293-1373	...	XR	...	60

TABLE 1. (Contd.)

Compound	Crystal systems	Axis	T_0, K	A	B	C	Range of temp, K^a	Accuracy	Method	Remarks	Reference
Lithium niobate $LiNbO_3$	Tri-gonal	c	273	3.0	0.0	0.0	273-473	...	XR	Ferroelectric	61
		a	273	12.0	0.0	0.0	273-473	...	XR	...	61
		c	473	4.0	0.0	0.0	473-673	...	XR	...	61
		a	473	15.0	0.0	0.0	473-673	...	XR	...	61
		c	673	3.0	0.0	0.0	673-873	...	XR	...	61
		a	673	18.0	0.0	0.0	673-873	...	XR	...	61
		c	873	0.0	0.0	0.0	873-1073	...	XR	...	61
		a	873	19.0	0.0	0.0	873-1073	...	XR	...	61
		c	1073	-6.0	0.0	0.0	1073-1273	...	XR	...	61
		a	1073	26.0	0.0	0.0	1073-1273	...	XR	...	61
		c	1273	-9.0	0.0	0.0	1273-1373	...	XR	...	61
		a	1273	42.0	0.0	0.0	1273-1373	...	XR	...	61
		c	273	7.885	-154.0	0.0	298-573	...	XR	...	62
		b	272	15.655	9.8	0.0	298-573	...	XR	...	62
		a	273	14.045	14.2	0.0	298-573	...	XR	...	62
Magnesium carbonate $MgCO_3$	Hexa-gonal	c	313	21.3	33.9	0.0	293-343	1	I	...	11
		a	313	5.99	24.3	0.0	293-343	1	I	...	11
Manganese dioxide (β) (pyrolusite) MnO_2	Tetra-gonal	c	298	6.93	0.0	0.0	298-770	...	XR	...	63
		a	298	6.69	0.0	0.0	298-770	...	XR	...	63
Potassium dihydrogen arsenate KH_2AsO_4		c	273	30.56	65.4	146.5	298-423	...	XR	Ferroelectric	64
		a	273	15.87	109.3	-8.7	298-423	...	XR	...	64
		c	273	47.1	0.0	0.0	223-323	...	I	...	34
		a	273	24.2	0.0	0.0	223-323	...	I	...	34
Potassium dihydrogen phosphate KH_2PO_4	Tetra-gonal	c	273	34.3	0.0	0.0	123-293	...	XR	Ferroelectric	65
		a	273	21.6	0.0	0.0	123-293	...	XR	T_c = 123 K^i	65
		a	273	22.0	0.0	0.0	123-298	...	I	...	34
		c	273	39.2	0.0	0.0	123-298	...	I	...	34
		a	273	24.9	0.0	0.0	223-323	...	I	...	34
		c	273	44.0	0.0	0.0	223-323	...	I	...	34
Potassium iodate KIO_4	Tetra-gonal	c	273	43.73	52.4	1257.8	301-353	...	XR	...	66
		a	273	5.46	612.2	169.2	301-353	...	XR	...	66

TABLE 1. (Contd.)

Compound	Crystal systems	Axis	T_0, K	A	B	C	Range of temp, K[a]	Accuracy	Method	Remarks	Reference
Rhodium sesquioxide Rh_2O_3	Hexa-gonal	c	273	5.246	6.369	-0.00748	RT-1123	...	XR	Corundum structure	67
		a	273	5.350	1.281	-0.001133	RT-1123	...	XR		67
Rubidium dihydrogen arsenate RbH_2AsO_4	Tetra-gonal	c	273	46.88	0.0	0.0	293-388	...	XR	Ferroelectric	33
		a	273	21.32	0.0	0.0	293-388	...	XR	...	33
		c	273	49.5	0.0	0.0	223-323	...	I	...	34
		a	273	16.9	0.0	0.0	223-323	...	I	...	34
Rubidium dihydrogen phosphate RbH_2PO_4	Tetra-gonal	c	273	52.0	0.0	0.0	303-351	...	XR	Ferroelectric	68
		a	273	27.75	0.0	0.0	303-351	...	XR	...	68
Ruthenium dioxide RuO_2	Tetra-gonal	c	...	-0.1	...	...	at 298	...	XR	...	53
		c	...	-5.7	...	...	at 923	...	XR	...	53
		a	...	10.6	...	...	at 298	...	XR	...	53
		a	...	14.4	...	...	at 923	...	XR	...	53
Scandium borate $ScBO_3$	Tri-gonal	a	273	1.143	3.580	0.2581	323-923	...	XR	...	69
		c	273	9.499	8.945	-0.1418	323-923	...	XR	...	69
Silicate oxy-apatite	Tri-gonal	a	...	6.6	...	...	at 300	...	...	[$Ca_{10}O(PO_4)_6$ is oxy-apatite]	70
		c	...	8.9	...	...	at 300	...	...		70
Silicon dioxide (quartz) SiO_2	Hexa-gonal	c	273	13.795	4.02	6.93	303-773	...	PR[m]	(Synthetic crystal)	71
		a	273	7.687	4.12	3.81	303-773	...	PR	...	71
		c	273	7.40	9.48	2.31	293-570	0.5	I	...	72
		a	273	13.35	18.00	2.76	293-570	0.5	I	...	72
		c	273	5.13	18.8	0.0	298-770	...	XR	Alpha-quartz[k]	73
		a	273	8.78	40.8	0.0	298-770	...	XR	Alpha-quartz[k]	73
		c	273	7.067	16.724	0.0	273-633	1	I	...	74
		a	273	13.246	25.25	0.0	283-607	...	...	...	75
		c	273	7.067	21.11	0.0	173-310	3	I	...	76
		c	631	25.80	-108.1	20.163	633-723	3	I	...	76
Titanium dioxide (anatase (TiO_2)	Tetra-gonal	c	273	7.380	6.620	1.771	300-985	3	XR	...	77
		a	273	3.533	5.610	0.4315	300-985	3	XR	...	77
		c	313	8.19	31.1	0.0	293-323	1	I	...	78
		a	313	4.68	29.5	0.0	293-323	1	I	...	78

TABLE 1. (Contd.)

Compound	Crystal systems	Axis	T_0, K	A	B	C	Range of temp, K[a]	Accuracy	Method	Remarks	Reference
Titanium dioxide (rutile) TiO_2	Tetragonal	c	313	9.19	22.5	0.0	293-343	1	I	...	79
		a	313	7.14	11.0	0.0	293-343	1	I	...	79
Zirconium silicate $ZrSiO_4$	Tetragonal	c	298	7.6	0.0	0.0	298-1573	...	XR	...	80
		a	298	4.4	0.0	0.0	293-1573	...	XR	...	80
Chrysoberyl $BeAl_2O_4$	Orthorhombic	a	313	5.16	12.2	0.0	293-343	1	I	...	11
		b	313	6.01	10.1	0.0	293-343	1	I	...	11
		c	313	6.02	22.0	0.0	293-343	1	I	...	11
Potassium nitrate KNO_3	Orthorhombic	c	273	20.1	0.0	0.0	103-293	...	XR	...	81
		a	273	22.0	0.0	0.0	303-373	...	XR	...	82
		b	273	23.5	0.0	0.0	303-373	...	XR	...	82
		c	273	182.6	0.0	0.0	303-373	...	XR	...	82
Titanium dioxide (brookite) TiO_2	Orthorhombic	a	...	14.494	...	...	at 290.5	1	I	...	78
		b	...	19.203	...	...	at 290.5	1	I	...	78
		c	...	22.049	...	...	at 290.5	1	I	...	78
Topaz $Al_2Fe_2SiO_4$	Orthorhombic	a	273	4.14	16.8	0.0	293-343	1	I	...	83
		b	273	4.84	15.3	0.0	293-343	1	I	...	83
		c	273	5.92	18.3	0.0	293-343	1	I	...	83
Tungsten trioxide WO_3	Orthorhombic	*	273	15.3	0.0	0.0	303-623	...	OL[n]	Ferroelectric	84
		*	273	12.5	0.0	0.0	623-873	...	OL	T_c = 983 K	84
		*	273	13.0	0.0	0.0	300-603	...		...	85
		*	273	10.0	0.0	0.0	623-983	...		...	85
		a	313	13.0	0.0	0.0	300-573	...	XR	...	86
		b	313	14.0	0.0	0.0	300-573	...	XR	...	86
		c	313	14.0	0.0	0.0	300-573	...	XR	...	86
		a	573	17.0	0.0	0.0	573-973	...	XR	...	86
		b	573	-1.3	0.0	0.0	573-973	...	XR	...	86
		c	573	18.0	0.0	0.0	573-973	...	XR	...	86

TABLE 1. (Contd.)

Compound	Crystal systems	Axis	T_0, K	A	B	C	Range of temp, K[a]	Accuracy	Method	Remarks	Reference
Mica $KH_2Al_2Si_3AlO_{12}$ or $KAl_2[(OH,F)_2 \times |AlSi_3O_{10}]$	Mono-clinic	a	...	8.1	...	...	at 324	1	I	Muscovite	87
		b	...	7.5	...	...	at 324	1	I	Muscovite	87
		Clea-	...	8.5	...	...	273-373	1	I	Muscovite	87
		vage plane[o]	...	13.5	...	...	273-373	1	I	Phlogopite (Al_2 is replaced by Mg_2)	87
Zirconium oxide (baddeleyite) ZrO_2	Mono-clinic	1	...	7.4	...	...	493-670	...	XR	...	88
		2	...	-0.7	...	...	493-670	...	XR	...	88
		3	...	16.3	...	...	493-670	...	XR	$\emptyset$ = 29°	88
		11	...	8.5	...	...	493-670	...	XR	to [100]	88
		33	...	14.2	...	...	493-670	...	XR	to [001]	88
Copper sulphate $CuSO_4 \cdot 5H_2O$	Tri-clinic	1	...	29.27	...	...	≈300	1	I	...	89
		2	...	41.58	...	...	≈300	1	I	$\emptyset$ = ?	89
		3	...	4.45	...	...	≈300	1	I	...	89

[a] Temperature range at which expansion coefficient is valid.
[b] 1, 2, 3, etc., = subscripts of the principal expansion coefficients.
[c] Interferometer.
[d] Error in the value of Π is given.
[e] X-ray.
[f] Pycnometer.
[g] a, b, c = Crystallographic a-, b-, c-axes.
[h] Denotes that the constants have been obtained from equations $a_t = b_0 + b_1 t + b_2 t + b_3 t^3$ or $\frac{\Delta a}{a}$ (%) = a', + b't + c't^3.
[i] Critical temperature.
[j] Quartz dilatometer.
[k] Computed by least squares procedure. b_0, b_1 ··· b_3 are constants and a', b', and c' are constants. The best representative curve fitted the equation.
[l] Three terminal capacitance.
[m] Push-rod method.
[n] Optic lever.
[o] Perpendicular cleavage plane.

TABLE 2. Coefficients of Thermal Expansion at Very Low Temperatures of Solids.

Compound, silica	Lattice, $D(10^{-11}/K^4)$	Temperature range, K	Method	Reference
Spectrosil 1000	-41 ± 1	1.5-10	3T-C	90
Spectrosil 1400	-35 ± 2	1.5-10	3T-C	90
Vitreosil 1000	-40 ± 1	1.5-10	3T-C	90
Vitreosil 1400	-35 ± 1	1.5-10	3T-C	90

A variety of factors including material impurities, crystalline defects, or sample preparation may lead to the disagreement between thermal expansion studies. However, even in well-crystallized pure compounds, such as MgO or Al_2O_3, a considerable range of published expansion coefficients exist. It appears that systematic experimental errors are very common in thermal expansion measurements, therefore, standardized procedures are needed to increase the accuracy of these studies. Until standardized procedures are developed, the accuracy of any given study must be conservatively accepted as no better than ±5%.

In Tables 1 and 2, the column labeled Compound lists the formula name and composition of both naturally occurring minerals and synthetic oxides. The second column in Table 1, labeled Crystal systems, lists the structure type. The temperature at which the measurement was made (T_0) is in kelvin units. The columns labeled A, B, and C are the values that are needed to solve equations 2 or 3 for the linear thermal expansion coefficient. The eighth column, Range of temp, K, indicates the temperature range for which the given data is applicable.

The compounds reported in Tables 1 and 2 have not been classified in any way. However, most of the compounds are arranged according to the crystal systems to which they belong. In the case of anisotropic crystals, the direction of measurement in the crystal is indicated in the column labeled Axis. Some solids listed have only α at a particular temperature; this is a reflection of what appears in the literature.

In Table 2, coefficients of thermal expansion at very low temperatures are listed for some commonly used silica glasses. A capacitance technique was used to make these measurements. In the capacitance dilatometer, the specimen dilates, thus altering the distance between the plates of the condenser producing variations in capacity. A three-terminal capacitance method is used to measure detection of movements as small as 10^{-9} cm and 10^{-10} cm; this allows measurements of α to be within an error of $\approx 10^{-10}$/K. A detailed description of this method is reported by White (Reference 91).

Table 3 lists thermal expansion of fixed-structure and simple structure compounds for which bond thermal expansion is equal to bulk linear expansion.

In a fixed-structure compound, the specific cations and anions fix the structure, while a simple structure compound (e.g., $Mg_{0.33}Fe_{0.67}O$) is one in which there is only one cation and one anion (e.g., NiO). The first column lists the compound type, followed by the bond and structure type. Z_c is the cation valence, Z_a is the anion valence, and n is the coordination number. The expansion coefficient $\bar{\alpha}^*_{1000}$ can be calculated by the following equation.

$$\bar{\alpha}^*_{1000} = \frac{2}{d_0 + d_{1000}} \left(\frac{d_{1000} - d_0}{980}\right) \approx \alpha_{510} \qquad (4)$$

where

d_0 = mean cation-anion bond distance at 20°C
d_{1000} = mean cation-anion bond distance at 1000°C

Table 4 lists polyhedral thermal expansion coefficients, taking into consideration the variation of isotropic temperature parameters and bonding parameters from complete three-dimensional, high-temperature (>400°C) crystal structure refinements.

Attempts have been made to relate thermal expansion to bonding parameters or other physical properties. Cameron and others related expansion coefficients of metal-oxygen bonds to bond strengths (Reference 132) where the expansion coefficient

$$\alpha = 4\nu\mu\pi^2C^2 \qquad (5)$$

where

α = expansion coefficient
ν = M-O stretching frequency
μ = reduced mass
C = speed of light

Although their relationship successfully modeled the bond expansion of their study, the Cameron equation does not predict many of the features of Tables 3 and 4. Cameron's equation does not predict that compounds having the rock salt-type structure such as Ni-O, Mg-O, Fe-O, and Ba-O

TABLE 3. Thermal Expansion of Fixed-Structure and Simple-Structure Compounds for Which Bond Thermal Expansion is Equal to Bulk Linear Expansion (Reference 92).

Compound	Bond	Structure Type	z_c	z_a	d(Å)	n	$\alpha^*_{1000} \times 10^{-6}$ (K^{-1})	Reference
NiO	Ni-O	NaCl	2	2	2.08	6	13.5	21
NiO	Ni-O	NaCl	2	2	2.08	6	16.7	93
MgO	Mg-O	NaCl	2	2	2.10	6	13.8	94
MgO	Mg-O	NaCl	2	2	2.10	6	12.7	95
MgO	Mg-O	NaCl	2	2	2.10	6	13.3	96
MgO	Mg-O	NaCl	2	2	2.10	6	12.7	97
MgO	Mg-O	NaCl	2	2	2.10	6	12.4	98
$(Mg_{33}Fe_{67})O$	(Mg, Fe)–O	NaCl	2	2	2.14	6	14.4	99
$(Mg_{37}Fe_{63})O$	(Mg, Fe)–O	NaCl	2	2	2.14	6	13.1	100
$(Mg_{64}Fe_{35})O$	(Mg, Fe)–O	NaCl	2	2	2.12	6	13.5	100
$(Mg_{84}Fe_{16})O$	(Mg, Fe)–O	NaCl	2	2	2.11	6	13.5	100
FeO	Fe–O	NaCl	2	2	2.16	6	12.2	100
FeO	Fe–O	NaCl	2	2	2.16	6	15.2	99
CoO	Co–O	NaCl	2	2	2.13	6	13.8	101
MnO	Mn–O	NaCl	2	2	2.22	6	14.1	102
CdO	Cd–O	NaCl	2	2	2.35	6	13.4	103
CdO	Cd–O	NaCl	2	2	2.35	6	13.2	104
CaO	Ca–O	NaCl	2	2	2.41	6	13.0	96
CaO	Ca–O	NaCl	2	2	2.41	6	13.6	105
SrO	Sr–O	NaCl	2	2	2.58	6	13.7	96
BaO	Ba–O	NaCl	2	2	2.77	6	17.8	106
BaO	Ba–O	NaCl	2	2	2.77	6	12.8	107

Reprinted by permission of John Wiley & Sons.

TABLE 3. (Contd.)

Compound	Bond	Structure Type	z_c	z_a	d(Å)	n	$\bar{a}^{*}_{1000} \times 10^{-6}$ (K^{-1})	Reference
BeO	Be–O	Zincite	2	2	1.66	4	8.4	96
BeO	Be–O	Zincite	2	2	1.66	4	9.1	105
ZnO	Zn–O	Zincite	2	2	1.80	4	6.8	96
ZnO	Zn–O	Zincite	2	2	1.80	4	7.7	103
Al_2O_3	Al–O	Corundum	3	2	1.91	6	8.4	94
Al_2O_3	Al–O	Corundum	3	2	1.91	6	9.3	96
Al_2O_3	Al–O	Corundum	3	2	1.91	6	8.6	105
Al_2O_3	Al–O	Corundum	3	2	1.91	6	8.1	108
Fe_2O_3	Fe–O	Corundum	3	2	2.03	6	10.3	15
Bi_2O_3	Bi–O	Bismite	3	2	2.44	6	9.4	103
Cr_2O_3	Cr–O	Corundum	3	2	1.99	6	7.2	100
Cr_2O_3	Cr–O	Corundum	3	2	1.99	6	7.9	102
UO_2	U–O	Fluorite	4	2	2.37	8	10.6	109
ThO_2	Th–O	Fluorite	4	2	2.42	8	9.3	109
ThO_2	Th–O	Fluorite	4	2	2.42	8	8.2	95
ThO_2	Th–O	Fluorite	4	2	2.42	8	9.6	105
CeO_2	Ce–O	Fluorite	4	2	2.34	8	12.6	110
ZrO_2	Zr–O	Baddeleyite	4	2	2.16	7	8.0	94
ZrO_2	Zr–O	Baddeleyite	4	2	2.16	7	8.4	101
HfO_2	Hf–O	Baddeleyite	4	2	2.17	7	7.1	105
β-SiO_2	Si–O	β Quartz	4	2	1.61	4	0.0	111
ReO_3	Re–O	ReO_3	6	2	1.87	6	1.1	112
LiF	Li–F	NaCl	1	1	2.02	6	46	113
NaF	Na–F	NaCl	1	1	2.31	6	45	114

TABLE 3. (Contd.)

Compound	Bond	Structure Type	z_c	z_a	$d(\mathring{A})$	n	$\dot{\alpha}^*_{1000} \times 10^{-6}$ (K^{-1})	Reference
NaCl	Na-Cl	NaCl	1	1	2.82	6	51	113
NaCl	Na-Cl	NaCl	1	1	2.82	6	55	114
KCl	K-Cl	NaCl	1	1	3.15	6	46	114
KCl	K-Cl	NaCl	1	1	3.15	6	51	114
KBr	K-Br	NaCl	1	1	3.26	6	45	115
KBr	K-Br	NaCl	1	1	3.26	6	49	113
RbBr	RB-Br	NaCl	1	1	3.43	6	44	115
KI	K-I	NaCl	1	1	3.53	6	47	113
CsBr	Cs-Br	CsCl	1	1	3.71	8	68	114
CaF_2	Ca-F	CaF_2	2	1	2.36	8	21	116
CaF_2	Ca-F	CaF_2	2	1	2.35	8	22	117
MnS	Mn-S	NaCl	2	2	2.61	6	18	102
PbS	Pb-S	NaCl	2	2	2.97	6	22	118
ZnS	Zn-S	Cubic ZnS	2	2	2.34	4	9	118
ZnS	Zn-S	Hex. ZnS	2	2	2.24	4	10	118
PbTe	Pb-Te	NaCl	2	2	3.23	6	20	119
PbSe	Pb-Se	NaCl	2	2	3.06	6	21	113
ZnSe	Zn-Se	Cubic ZnS	2	2	2.45	4	9	118
AlAs	Al-As	Cubic ZnS	3	3	2.43	4	5.3	120
GaAs	Ga-As	Cubic ZnS	3	3	2.45	4	6.7	121
TiN	Ti-N	NaCl	4	4	2.12	6	9.4	102
BN	B-N	Cubic ZnS	3	3	1.45	4	13.0	122
UN	U-N	NaCl	4	4	2.44	6	8.6	109
NbC	Nb-C	NaCl	4	4	2.23	6	7	123
TaC	Ta-C	NaCl	4	4	2.23	6	7	123
TiC	Ti-C	NaCl	4	4	2.16	6	8	113
ZrC	Zr-C	NaCl	4	4	2.34	6	7	113
C	C-C	Diamond	4	4	1.54	4	3.5	95

NOTE:

$$^*\dot{\alpha}_{1000} = \frac{2}{d_0 + d_{1000}} \left(\frac{d_{1000} - d_0}{980} \right) \approx \alpha_{510},$$

where d_0 and d_{1000} are mean cation-anion bond distance at 20°C and 1000°C, respectively.

TABLE 4. Polyhedral Thermal Expansion, Variation of Isotropic Temperature Parameters and Bonding Parameters From Complete Three-Dimensional, High-Temperature (≥400°C) Crystal Structure Refinements (Reference 92).

Bond	Structure	Site	Formula	Mineral Name	z_c	z_a	d(Å)	n	$\dot{\alpha}^*_{1000} \times 10^6$ (K^{-1})	$\partial B/\partial T$ (Å^2/K)	Reference
Mg-O	NaCl		MgO	Periclase	2	2	2.106	6	12.4(1)	0.0017(1)	98
V-O	Corundum		V_2O_3	Karelianite	3	2	2.010	6	13(1)	0.0008(1)	124
Ti-O	Corundum		Ti_2O_3		3	2	2.046	6	8(1)	0.0010(1)	125
Si-O	Cristobalite		SiO_2	Cristobalite	4	2	1.609	4	0(4)	0.0007(4)	126
Ti-O	Rutile		TiO_2	Rutile	4	2	1.959	6	8(1)	0.0014(1)	127
Ti-O	Brookite		TiO_2	Brookite	4	2	1.960	6	6(2)	0.0014(1)	127
Ti-O	Anatase		TiO_2	Anatase	4	2	1.949	6	8(1)	0.0016(1)	128
Mg-O	Garnet		$Mg_3Al_2Si_3O_{12}$	Pyrope	2	2	2.269	8	13(1)	0.0020(1)	129
Al-O					3	2	1.887	6	7(1)	0.0009(2)	129
Si-O					4	2	1.635	4	2(2)	0.0006(1)	129
Ca-O	Garnet		$Ca_3Al_2Si_3O_{12}$	Grossular	2	2	2.406	8	10(1)	0.0012(1)	129
Al-O					3	2	1.921	6	10(1)	0.0008(1)	129
Si-O					4	2	1.647	4	6(2)	0.0010(3)	129
Mg-O	Olivine	M1	Mg_2SiO_4	Forsterite	2	2	2.095	6	16(3)	0.0015(1)	130
Mg-O		M2			2	2	2.133	6	16(2)	0.0015(1)	130
Si-O		T			4	2	1.630	4	−1(3)	0.0009(1)	130
(Mg, Fe)-O	Olivine	M1	$(Mg_{1.4}Fe_{0.6})SiO_4$	Hortonolite	2	2	2.118	6	12(1)	0.0016(1)	131
(Mg, Fe)-O		M2			2	2	2.148	6	12(1)	0.0014(1)	131
Si-O		T			4	2	1.638	4	−1(1)	0.0009(1)	131
(Fe, Mg)-O	Olivine	M1	$(Mg_{0.75}Fe_{1.10}Mn_{0.15})SiO_4$	Hortonolite	2	2	2.135	6	16(4)	0.0015(1)	132
(Fe, Mg)-O		M2			2	2	2.167	6	14(3)	0.0015(1)	132
Si-O		T			4	2	1.629	4	2(3)	0.0009(1)	132
Fe-O	Olivine	M1	Fe_2SiO_4	Fayalite	2	2	2.157	6	12(1)	0.0032(2)	133
Fe-O		M2			2	2	2.179	6	14(1)	0.0028(2)	133
Si-O		T			4	2	1.628	4	−4(3)	0.0018(2)	133

Reprinted by permission of John Wiley & Sons.

TABLE 4. (Contd.)

Bond	Structure	Site	Formula	Mineral Name	z_c	z_a	d(Å)	n	$\bar{\alpha}^{*}_{1000} \times 10^6$ (K^{-1})	$\partial B/\partial T$ (Å^2/K)	Reference
Ni-O	Olivine	M1	Ni_2SiO_4	Ni olivine	2	2	2.078	6	15(1)	0.0012(1)	127
Ni-O		M2			2	2	2.100	6	13(1)	0.0013(1)	127
Si-O		T			4	2	1.639	4	0(1)	0.0008(1)	127
Ca-O	Olivine	M1	$CaMgSiO_4$	Monticellite	2	2	2.129	6	18(1)	0.0020(2)	127
(Mg, Fe)-O		M2			2	2	2.368	6	13(1)	0.0019(2)	127
Si-O		T			4	2	1.637	4	−3(3)	0.0015(1)	127
Ca-O	Olivine	M1	$Ca(Mn_{0.85}Mg_{0.10}Zn_{0.05})SiO_4$	Glaucochroite	2	2	2.210	6	15(1)	0.0025(1)	127
(Mn, Mg)-O		M2			2	2	2.366	6	15(1)	0.0019(1)	127
Si-O		T			4	2	1.640	4	−7(3)	0.0017(1)	127
Ni-O	Spinel	M	Ni_2SiO_4		2	2	2.060	6	13(1)	0.0012(1)	134
Si-O		T			4	2	1.660	4	1(4)	0.0009(1)	134
Ca-O	Sphene		$CaTiSiO_5$	Sphene	2	2	2.450	7	16(3)	0.0024(1)	135
Ti-O					4	2	1.956	6	9(2)	0.0012(2)	135
Si-O					4	2	1.639	4	0(2)	0.0007(1)	135
(Fe, Mg)-O	Pseudobrookite		$(Fe, Mg)Ti_2O_5$	Armalcolite	2	2	2.103	6	−11(3) †	0.0014(1)	136
Ti-O					4	2	1.979	6	22(2)	0.0014(1)	136
Pb-O	Perovskite		$PbTiO_3$		2	2	2.843	12	23(8) ‡	0.0038(2)	137
Ti-O					4	2	2.013	6	20(10)	0.0012(6)	137
Fe-O	Orthopyroxene	M1	$FeSiO_3$	Orthoferrosilite	2	2	2.135	6	16(1) §	0.0018(1)	138
Fe-O		M2			2	2	2.352	7	24(2)	0.0025(1)	138
Si-O		SiA			4	2	1.626	4	−3(1)	0.0012(1)	138
Si-O		SiB			4	2	1.637	4	−7(1)	0.0012(1)	138
(Mg, Fe)-O	Orthopyroxene	M1	$(Mg_{.3}Fe_{.7})SiO_3$	Ferrohypersthene	2	2	2.104	6	20(2) §	0.0020(1)	139
Fe-O		M2			2	2	2.340	7	18(2)	0.0030(1)	139
Si-O		SiA			4	2	1.628	4	−3(1)	0.0018(1)	139
Si-O		SiB			4	2	1.637	4	−16(2)	0.0019(1)	139
(Mg, Fe)-O	Clinopyroxene (2 chain)	M1	$(Mg_{.3}Fe_{.7})SiO_3$	Clinohypersthene	2	2	2.111	6	16(2) †	0.0020(2)	140
Fe-O		M2			2	2	2.297	7	−2(4)	0.0026(1)	140
Si-O		SiA			4	2	1.625	4	−5(5) §	0.0015(2)	140
Si-O		SiB			4	2	1.640	4	−24(4)	0.0020(2)	140

TABLE 4. (Contd.)

Bond	Structure	Site	Formula	Mineral Name	z_c	z_a	d(Å)	n	$\bar{\alpha}^*_{100u} \times 10^6$ (K^{-1})	$\partial B/\partial T$ (Å^2/K)	Reference
Al-O	Clinopyroxene	M1	$LiAlSi_2O_6$	Spodumene	3	2	1.919	6	10(1)	0.0012(1)	141
Li-O		M2			1	2	2.211	6	20(1)	0.0041(1)	141
Si-O		T			4	2	1.618	4	1(1)	0.0011(1)	141
Fe-O	Clinopyroxene	M1	$NaFe^{3+}Si_2O_6$	Acmite	3	2	2.025	6	8(1)	0.0012(1)	141
Na-O		M2			1	2	2.518	8	13(1)	0.0034(1)	141
SiO		T			4	2	1.628	4	1(1)	0.0011(1)	141
Al-O	Clinopyroxene	M1	$NaAlSi_2O_6$	Jadeite	3	2	1.929	6	10(1)	0.0009(1)	141
Na-O		M2			1	2	2.469	8	13(1)	0.0026(1)	141
Si-O		T			4	2	1.625	4	1(1)	0.0008(1)	141
Cr-O	Clinopyroxene	M1	$NaCrSi_2O_6$	Ureyite	3	2	1.988	6	6(1)	0.0008(1)	141
Na-O		M2			1	2	2.489	8	13(1)	0.0029(1)	141
Si-O		T			4	2	1.624	4	2(2)	0.0009(1)	141
Fe-O	Clinopyroxene	M1	$CaFeSi_2O_6$	Hedenbergite	2	2	2.130	6	10(1)	0.0015(1)	141
Ca-O		M2			2	2	2.511	8	16(1)	0.0022(1)	141
Si-O		T			4	2	1.635	4	0(1)	0.0010(1)	141
Mg-O	Clinopyroxene	M1	$CaMgSi_2O_6$	Diopside	2	2	2.077	6	14(1)	0.0016(1)	141
Ca-O		M2			2	2	2.498	8	16(1)	0.0023(1)	141
Si-O		T			4	2	1.635	4	1(1)	0.0011(1)	141
Na-O	Feldspar	Na	$NaAlSi_3O_8$	High albite	1	2	2.807	9	17(1)	0.0046(2)	142
$(Al_{.25}Si_{.75})$-O		T_{1o}			3.75	2	1.646	4	−1(1)	0.0015(1)	142
$(Al_{.25}Si_{.75})$-O		T_{1m}			3.75	2	1.641	4	1(1)	0.0015(1)	142
$(Al_{.25}Si_{.75})$-O		T_{2o}			3.75	2	1.641	4	−3(1)	0.0015(1)	142
$(Al_{.25}Si_{.75})$-O		T_{2m}			3.75	2	1.642	4	−4(1)	0.0015(1)	142
Na-O	Feldspar	Na	$NaAlSi_3O_8$	High albite	1	2	2.807	9	18(1)	0.0045(1)	143
$(Al_{.25}Si_{.75})$-O		T_{1o}			3.75	2	1.649	4	−3(1)	0.0015(1)	143
$(Al_{.25}Si_{.75})$-O		T_{1m}			3.75	2	1.642	4	0(1)	0.0015(1)	143
$(Al_{.25}Si_{.75})$-O		T_{2o}			3.75	2	1.640	4	0(1)	0.0015(1)	143
$(Al_{.25}Si_{.75})$-O		T_{2m}			3.75	2	1.642	4	−1(1)	0.0015(1)	143

TABLE 4. (Contd.)

Bond	Structure	Site	Formula	Mineral Name	z_c	z_a	d(Å)	n	$\bar{\alpha}^{*}_{1000} \times 10^6$ (K^{-1})	$\partial B/\partial T$ (Å^3/K)	Reference
Na-O	Feldspar	Na	$NaAlSi_3O_8$	Low albite	1	2	2.634	7	35(2)	0.0082(1)	144
Al-O		T_{1o}			3	2	1.740	4	0(1)	0.0017(1)	144
Si-O		T_{1m}			4	2	1.609	4	−2(1)	0.0015(1)	144
Si-O		T_{1o}			4	2	1.614	4	−2(1)	0.0016(1)	144
Si-O		T_{1m}			4	2	1.615	4	−1(1)	0.0016(1)	144
Ca-O	Feldspar		$CaAl_2Si_2O_8$	Anorthite	2	2	2.493	7	36(7)	0.0021(5)	145
Al-O					3	2	1.747	4	−8(6) †	0.0008(2)	145
Si-O					4	2	1.614	4	13(6)	0.0006(2)	145
Na-O	Nepheline		$(Na_{5.4}Ca_{0.4}K_{1.3}\square_{0.3})Al_8Si_8O_{32}$	Nepheline	1	2	2.62	8	48(4)	0.0052(4)	146
Na-O	Zeolite		$Na_2Al_2Si_3O_{10} \cdot 2H_2O$	Natrolite	1	2	2.445	6	17(1)	0.0011(2)	125
(Mg, Fe)-O	Cordierite	M	$(Mg_{1.9}Fe_{0.1})(Si_5Al_4)O_{18}(M_2O)_{0.56}$	Cordierite	2	2	2.108	6	13(1)	0.0015(1)	147
Al-O		T_11			3	2	1.758	4	−3(3)	0.0012(1)	147
Al-O		T_16			3	2	1.742	4	3(3)	0.0011(1)	147
Si-O		T_26			4	1	1.626	4	4(3)	0.0010(1)	147
Si-O		T_21			4	2	1.614	4	0(3)	0.0009(1)	147
Si-O		T_23			4	2	1.617	4	1(1)	0.0009(1)	147
K-O	Mica	K	$KMg_3AlSi_3O_{10}(OH)_2$	Phlogopite	1	2	2.987	6	21(4)	0.0064(5)	148
Mg-O		M_1			2	1.67	2.056	6	9(6)	0.0018(2)	148
Mg-O		M_2			2	1.67	2.070	6	17(6)	0.0025(2)	148
$(Al_{.25}Si_{.75})$-O		T			3.75	2	1.651	4	−5(5)	0.0022(2)	148
Al-O	Sillimanite	Al1	Al_2SiO_5	Sillimanite	3	2	1.912	6	7(2)	0.0009(1)	149
Al-O		Al2			3	2	1.763	4	3(2)	0.0009(1)	149
Si-O		Si			4	2	1.627	4	1(1)	0.0008(1)	149
Al-O	Andalusite	Al1	Al_2SiO_5	Andalusite	3	2	1.935	6	12(1)	0.0013(1)	149
Al-O		Al2			3	2	1.836	5	6(1)	0.0008(1)	149
Si-O		Si			4	2	1.631	4	0(1)	0.0007(1)	149
Al-O	Kyanite	Al1	Al_2SiO_5	Kyanite	3	2	1.902	6	11(1)	0.0010(1)	149
Al-O		Al2			3	2	1.913	6	9(1)	0.0010(1)	149
Al-O		Al3			3	2	1.919	6	9(2)	0.0010(1)	149
Al-O		Al4			3	2	1.896	6	10(1)	0.0010(1)	149
Si-O		Si1			4	2	1.635	4	2(2)	0.0007(1)	149
Si-O		Si2			4	2	1.636	4	3(2)	0.0007(1)	149

TABLE 4. (Contd.)

Bond	Structure	Site	Formula	Mineral Name	z_c	z_a	d(Å)	n	$\bar{\alpha}^*_{1000} \times 10^6$ (K^{-1})	$\partial B/\partial T$ (Å^2/K)	Reference
Li–O	Stuffed Quartz	Li1	$LiAlSiO_4$	β Eucryptite	1	2	1.964	4	19(8)	-	150
Li–O		Li2			1	2	2.080	4	16(10)		150
Li–O		Li3			1	2	2.017	4	31(13)	0.0060(10)	150
Al–O		Al1			3	2	1.752	4	-2(4)	0.0016(2)	150
Al–O		Al2			3	2	1.713	4	4(6)	0.0018(2)	150
Si–O		Si1			4	2	1.640	4	5(5)	0.0010(1)	150
Si–O		Si2			4	2	1.594	4	8(8)	0.0009(1)	150
Mg–O	Amphibole	M1	$Ca_2Mg_5Si_8O_{22}(OH)_2$	Tremolite	2	2	2.075	6	13(1)	0.0016(1)	151
Mg–O		M2			2	2	2.077	6	15(2)	0.0016(1)	151
Mg–O		M3			2	2	2.066	6	12(1)	0.0015(1)	151
Ca–O		M4			2	2	2.506	8	16(1)	0.0025(1)	151
Si–O		T1			4	2	1.620	4	0(1)	0.0014(1)	151
Si–O		T2			4	2	1.632	4	2(1)	0.0014(1)	151
Ba–O	Perovskite	Ba	$Ba_2Bi^{3+}Bi^{5+}O_6$		2	2	3.07	12	15(3)	0.0032(3)	152
Bi–O		Bi1			3	2	2.28	6	10(6)	0.0022(4)	152
Bi–O		Bi2			5	2	2.12	6	0(2)	0.0000(5)	152

$$* \; \alpha_{1000} = \frac{2}{d_0 + d_{1000}} \cdot \left(\frac{d_{1000} - d_0}{980} \right) \approx \alpha_{510},$$

where d_0 and d_{1000} are mean cation anion bond distance at 20°C and 1000°C, respectively

† These expansion coefficients are anomalous because of cation disordering at high temperature.

‡ Powder profile refinement.

§ These expansion coefficients are anomalous because of changes of structural topology at high temperature.

‖ Several high-temperature studies involving phases that undergo transitions have not been included because bond distance variations are not continuous versus temperature. The structure studies include $(Ca_{.1}Mg_{.4}Fe_{.5})$-pigeonite (Reference 153); Bi_2WO_6 (Reference 154); $MgSiO_3$-pyroxenes (References 155 and 156); $(Mg_{.3}Fe_{.7})SiO_3$-clinohypersthene (Reference 157); and $Mg_7Si_8O_{22}(OH)_2$-cummingtonite (Reference 158).

have similar expansion coefficients. The data in Tables 1 and 2 are measured values, while the data in Tables 3 and 4 are calculated values.

Some authors have attempted to relate thermal expansivity to other physical variables as was demonstrated by Hanneman and Gatos (Reference 159). The relation between compressibility and thermal expansion coefficients in cubic metals and alloys is that thermal expansion and compressibility are proportional for cubic metals and alloys. Van Uitert and others found a simple inverse relation between the coefficient of thermal expansion and the melting temperature for a large number of close-packed structures (References 160 and 161).

Many investigators have examined the relationships between thermal expansion, thermal vibration amplitudes, and specific heat. The number of attempts to predict thermal expansion and relate expansion to other physical variables attest to the usefulness that such relationships would be for modeling the high-temperature behavior of solid-state materials.

A few simple empirical relationships, which allow the prediction of bond distance changes with temperature, can be deduced from Tables 3 and 4. The first important observation is that all cation coordination polyhedra of a given type (i.e., silicon-oxygen tetrahedra, magnesium-oxygen octahedra) show similar expansion coefficients. For example, Tables 3 and 4 contain 48 compounds containing silicon tetrahedra that have coefficients near or equal to zero within two standard errors. Of the remaining five compounds, two tetrahedra have positive expansion coefficients. In the case of anorthite, the positive expansion of Si-O is accompanied by a large contraction of adjacent Al-O bonds. It seems that these anomalies are caused by disordering of Si and Al rather than changes in bonds of a fixed composition. The other three nonzero Si-O expansivities occur in the tetrahedral chains. In each of these tetrahedral sites, the bridging oxygen to silicon distance shows significant shortening with increasing temperature. Therefore, this anomalous behavior can be due to the changing topology of the material with temperature. The positive expansion in grossular garnet, is still a small, and possibly insignificant, expansion. All of the Mg-O thermal expansion coefficients are consistent with a value of $14 \times 10^{-6}\,{}^{\circ}C^{-1}$ (± 10).

An important conclusion that can be made from these observations is that the thermal expansion coefficient for each type of polyhedron is <u>independent of structural linkages</u> of the polyhedron, as long as the site chemistry and the nearest neighbor configuration of the structure do not change with temperature. Therefore, for each type of cation-oxygen polyhedron, a value for an expansion coefficient exists that may be used to predict behavior at high temperature. A second generalization evident from Table 4 is that all oxygen-based polyhedra with the same Pauling bond strength (cation valence, Z_c, divided by coordination number, n) have the same $\overline{\alpha}_{1000}$.

Bulk thermal expansion coefficients are not only a function of bond distance and bond strength, but also how these polyhedra are linked together. Two polyhedra may be linked by a shared face, a shared edge, a shared corner or merely by Van der Waal's forces. The type and distribution of these polyhedra linkages are the most important factors in determining the bulk thermal expansion of a compound. The most rigid polyhedral linkage is one in which polyhedra share faces or edges in three dimensions. For example, in the rock salt-, corundum-, spinel-, and garnet-type compounds in which a fully edge-linked structure exists, the bulk thermal expansion is small. The bulk thermal expansion is similar in magnitude to the thermal expansion of metal-oxygen polyhedra.

Table 5 lists a variety of nominally single phase oxides with very low ($<1 \times 10^{-6}/K^1$), low ($1\text{-}4 \times 10^{-6}/K$), and intermediate ($4\text{-}9 \times 10^{-6}/K$) thermal expansion coefficients (References 162 through 164).

Three expansion coefficients versus temperature plots are illustrated in Figure 1. These are materials that are commonly used as low-expansion materials in the temperature region of 0 to 600 K. As can be seen in this figure, the expansion coefficient is not constant as a function of temperature.

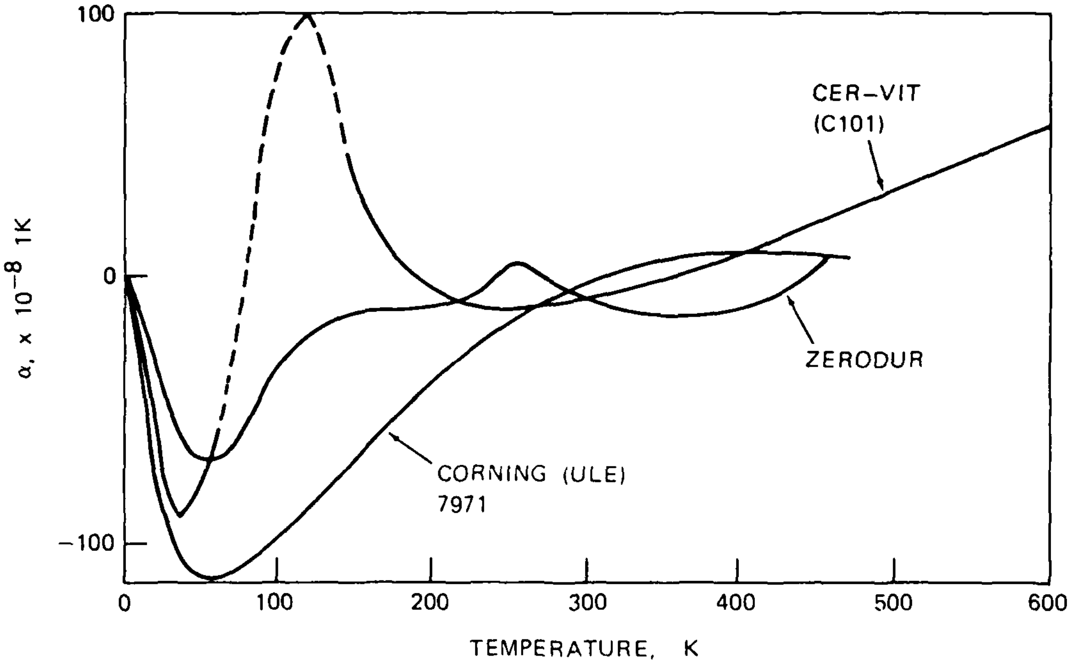

FIGURE 1. Expansion Coefficients Versus Temperature Plots for Some Commonly Used Laser Gyro Materials.

TABLE 5. Oxides With Very Low to Intermediate Thermal Expansion.

Material	$\alpha^{a} \times 10^{6}$ (K^{-1})	mp[b](K)	Porosity, %	Crystal system[c]	Reference
Very low					
$Ta_{16}W_{18}O_{94}$	-5.1	>2050	31	Tetragonal	162
Ta_2WO_8	-2 to 3.2	2125	1-36	Orthorhombic	162
$Nb_2Hf_6O_{17}$ (Solid solution) Nb_2O_5 (Solid solution)	-0.7	1700	38	---	163
$(Hf_{0.8}W_{0.8}Ta_{1.6})O_8$	0.0	1690	41	Orthorhombic Ta_2WO_8 type	163
$Hf_{1.26}Ti_{0.74}O_4$	0.0	>2475	16	Orthorhombic $HfTiO_4$ type	163
$Ta_{22}W_4O_{67}$	0.6	2150	40	Orthorhombic	162
Al_2TiO_5[d]	0.8	2060	12	Orthorhombic	163
Low					
$(Hf_{0.945}H_{0.315}Ti_{0.74})O_4$	2.2	2135	12	Orthorhombic $HfTiO_4$ type	163
$Zr_{1.71}Nb_{10.24}O_{29}$	2.5	1680	32	Orthorhombic $Ti_2Nb_{10}O_{29}$ type	163
$Hf_{1.71}Nb_{10.24}O_{29}$	3.2	1700	35	Orthorhombic $Ti_2Nb_{10}O_{29}$ type	163
Ta_2TiO_7	3.4	1920	36	Monoclinic	163
$HfTiO_4$	3.6	2455	29	Orthorhombic	163
Nb_2TiO_7	3.6	2155	2	Monoclinic	163
Intermediate					
$NiTa_2O_6$[e]	4.1	1965	18	Tetragonal	163
$Zr_{0.294}Ta_{1.765}O_5$	4.2	2000	36	Hexagonal δ-Ta_2O_5 type	163
$AlHfTaO_6$	4.4	2435	30	Orthorhombic	163
$AlTaO_4$[e]	5.0	1935	21	Hexagonal	163
$(Hf_{0.315}H_{0.315}Ti_{0.37})O_2$	5.9	>2625	5	Monoclinic HfO_2 type	163
$(Al_{0.76}Hf_{0.38}Zr_{0.38}Ti_{0.67})O_4$	6.4	1925	36	Orthorhombic $HfTiO_4$ type	163
$YHfTaO_6$	6.6	2185	13	Orthorhombic	164
$MgTa_2O_6$	6.8	2000	38	Tetragonal	163
$AlTiTaO_6$	7.1	1970	28	Tetragonal	164
$YTiTaO_6$	7.5	2025	28	Orthorhombic	163
Y_2TiO_5	8.8	2115	22	Orthorhombic	164

[a] Coefficient of thermal expansion assuming linear thermal expansion from 295-1275 K.

[b] Melting point values measured by differential thermal analysis.

[c] Single phase by X-ray diffraction.

[d] Sample contained some TiO_2 as a second phase as determined by X-ray diffraction.

[e] Sample contained some δ-Ta_2O_5 determined by X-ray diffraction.

CONCLUSIONS

This paper reports expansion coefficients for a variety of oxides and oxide ceramics and discusses some rules for predicting low expansion oxides. Some of the structure types in which low thermal expansion should be expected are rock salt, corundum, spinel, and garnet. This information can make it possible to synthesize new materials with somewhat predictable expansion coefficients. It is possible that a multiphase material can be engineered to have a net zero expansion at a given temperature by forming a ceramic composite with components that have both negative and positive expansion coefficients. This is the approach taken in Zerodur and in ULE, but clearly, some improvements need to be made. However, just having a powder that has the right composition to give a low expansion ceramic is only part of the problem. Studies have indicated that processing can drastically alter expansion properties of oxides. It has been found that fine-grained (<10 μm) anisotropic ceramic materials, such as hafnium oxide, hafnium titanate, and tantalum tungstate may exhibit thermal expansion hysteresis effects with minimal observable microcracking or grain boundary separations (References 165 through 167). In ceramic materials, thermal expansion hysteresis can be accounted for by reversible phase transitions or by microcracking.

For large-grained bodies of materials, microcracking is the common cause of thermal expansion hysteresis. Considering fine-grained materials data shows that all materials will have a critical grain size below which no observable microcracking can occur (Reference 168). However, fine-grained ceramic materials have a greater tendency to deform without cracking since mechanical strength is greater, and there is decreased localized grain-boundary stress resulting from thermal expansion anisotropy (Reference 169). Therefore, for ceramic materials, any effect of cyclic plastic deformation (strain induced from thermal cycling) should increase as the grain-size decreases.

Whenever thermal expansion hysteresis is apparent and phase transformations or microcracking are not apparent, hysteresis in the thermal expansion courses of ceramics could be accounted for by a plastic deformation component (caused by thermal stresses at polycrystalline grain boundary) added to the elastic strain (thermal expansion or contraction). Because of the factors that can affect the expansion coefficient of a material, synthesis of "low expansion" ($<10^{-8}$/K) materials for laser gyro, structural ceramic applications are an area of continuous research.

REFERENCES

1. R. S. Krishnan, R. Srinivasan, and S. Devanarayanan. *Thermal Expansion of Crystals*. New York, Pergamon Press, 1979. 305 pp.

2. A. Liberman and W. B. Gandall. "Design and Construction of a Self-Calibrating Dilatometer for High Temperature Use," *J. Amer. Ceram. Soc.,* **35** (1952), pp. 304-8.

3. P. Fischer, W. Schmidt, W. Bruchl, and G. Kuehan. "Lattice Constant of $Al_{0.8}$ $Ga_{0.2}$ As Between -110° and +90°C," *Krist. Tech.,* **7** (1972), pp. K5-K7.

4. C. Martinek and P. A. Hummel. "Linear Thermal Expansion of 3 Tungstates," *J. Amer. Chem. Soc.,* **51** (1968), pp. 227-28.

5. A. K. Streedhar. "Thermal Expansion of Crystals at Low Temperatures. Part II. Alums," *J. Indian Inst. Sci.,* **36** (1954), p. 182.

6. H. Fizeau. "Sur la Dilatation du Diamant et du Protonyde de Cuivre Crystallise Sons l'Influence de la Chaleur," *Acad. Sci. (Paris),* **60** (1865), p. 1161.

7. R. Srinivasan. "Thermal Expansion of Nitrates of Lead, Barium, and Strontium," in *Proceedings. Indian Academy of Science,* **A41**, 1955. Pp. 49-54.

8. O. Hulsmann and W. Bilz. "Uber die Thermische Ausdehnung Einiger Verbindungen und ihre Abschatzung nach der Grüneisenschen Regel," *Anorg. Allg. Chem.,* **219** (1934), p. 357.

9. P. Joho. "Prazisionsmessung der Gitter-Konstanten und des Ausdehnungs-Koeffizienten von Barium Titanate," *Z. Kristallogr.,* **120** (1964), pp. 329-41.

10. J. A. Bland. "The Thermal Expansion of Cubic $BaTiO_3$ From 350 to 1050°C," *Can. J. Phys.,* **37** (1959), pp. 417-21.

11. H. Fizeau. *"Annuaire pour l'an (1888), Paris, Bureau des Longitudes."*

12. V. N. Zharkov. "The Influence of Pressure on Anharmonicities," *Dokl. Akad. Nauk., SSSR* **154** (1964) pp. 302-5.

13. L. Iyengar, B. Ram Prasad and B. Qudri. "Thermal Expansion of Cobalt Ferrite and Cobalt Zinc Ferrite," *Curr. Sci.,* **42** (1973), pp. 534.

14. R. E. Mistler, G. L. Ploetz, and J. A. Smith. "Thermal Expansion of Polycrystalline La and N Sesquoxides," *J. Amer. Ceram. Soc.,* **46** (1963), pp. 561-62.

15. S. S. Sharma. "Thermal Expansion of Crystals: Part IV. Silver Chloride, Lithium Fluoride and Magnesium Oxide," *Proc. Indian Acad. Sci.,* **A32** (1950), pp. 268-74.

16. B. N. Dutta. "Lattice Constants and Thermal Expansion of MgO up to 878°C by X-ray Method," *J. Sci. Res. (Banaras Hindu Univ.) (India),* **15** (1964-65), pp. 80-85.

17. G. K. White and O. L. Anderson. "Grüneisen Parameter of MgO," *J. Appl. Phys.,* **37** (1966), pp. 430-32.

18. T. H. Nielsen and M. H. Leipold. "Thermal Expansion of Yttrium Oxide and of MgO with Y_2O_3," *J. Amer. Ceram. Soc.,* **47** (1964), p. 256.

19. S. S. Sharma. "Thermal Expansion of Crystals: II. Magnetite and Fluorite," *Proc. Indian Acad. Sci.,* **A31** (1950), pp. 261-74.

20. N. N. Zhuravlev and A. A. Stepanova. "X-Ray Determination of the Coefficients of Thermal Expansion of the Monosilicides of Mn and Co," *Atomnaya Energiya (USSR),* **13** (1962), pp. 183-84.

21. T. H. Nielson and M. H. Leipold. "Thermal Expansion of Nickel Oxide," *J. Amer. Ceram. Soc.,* **48** (1965), p. 164.

22. S. S. Sharma. "Thermal Expansion of Crystals: I. Sodium Chlorate and Sodium Bromate," *Proc. Indian Acad. Sci.,* **A31** (1950), pp. 83-94.

23. S. Ganesan. "Thermal Expansion of $NaClO_3$, $NaBrO_3$," *J. Indian Inst. Sci.,* **41** (1959), pp. 9-15.

24. J. B. Austin and R. H. H. Pierce, Jr. "The Linear Thermal Expansion of Sodium Tungstate Between 20° and 600°C," *J. Chem. Phys.* **3** (1935), p. 683.

25. H. Fizeau. "Sur la Dilatation des Corps Solides par la Chaleur," *C. R. Acad. Sci. (Paris),* **66** (1868), p. 1072.

26. H. Fizeau. "Ueber die Ausdehnung starrer Korper. Zweite Abhandlung." *Ann. Phys. Chem. (Leipzig),* **135** (1868), p. 372.

27. S. Devanarayanan and P. S. Narayanan. "Thermal Expansion of Strontium Titanate," *Indian J. Pure Appl. Phys.*, **6** (1968), pp. 714-15.

28. S. Devanarayanan. "Ferroelectric Crystals and Their Properties (Investigations on Thermal Expansion of Ferroelectrics)," *Ph.D. thesis submitted to the Indian Institute of Science, Bangalore-12*, (1969).

29. B. Alefeld. "The Change of Lattice Parameters of $SrTiO_3$ Near the Phase Transition Point at 108°K," *Z. Phys.*, **222** (1969), pp. 155-64.

30. S. Aronson, E. Cisney, and K. A. Gingerich. "Thermal Expansion of Some Cubic Refractory Compounds of Thorium," *J. Amer. Ceram. Soc.*, **50** (1967), pp. 248-52.

31. S. S. Sharma. "Thermal Expansion of Crystals: Part VI. Alumina," *Proc. Indian Acad. Sci.*, **A33**, (1951), pp. 245-49.

32. P. G. Strelkov, I. I. Lifanov, and N. G. Sherstyukov. "Mean Curves of Elongation Temperature Coefficients of Monocrystalline Quartz," *Meas. Tech.*, No. 9 (1966), pp. 1116-20.

33. V. T. Deshpande, A. A. Khan, and P. G. Pardiker. "Thermal Expansion of Rubidium Dihydrogen Arsenate," *Indian J. Pure Appl. Phys.*, **6** (1968), pp. 97-8.

34. W. R. Cook, Jr. "Thermal Expansion of Crystals with KH_2PO_4 Structure," *J. Appl. Phys.*, **38** (1967), pp. 1637-42.

35. V. Hovi, K. Paavola, and E. Nurmi. "X-Ray Investigation of the Modification I, II, and III of HN_4I and ND_4I at Temperatures Between 190° and -176°C," *Ann. Acad. Sci. Fennicae (Finland)*, **AVI**, No. 328 (1969), p. 8.

36. V. T. Deshpande and S. V. Suryanarayana. "Lattice Thermal Expansion of Barium Tungstate," *J. Appl. Phys.*, **41** (1970), p. 422.

37. B. Morosin. "Structure and Thermal Expansion of Beryl," *Acta Crystallogr.*, **B28** (1972), pp. 1899-903.

38. S. M. Lang. "The Axial Expansion of BeO Between Room Temperature and 1700°C," *Acta Crystallogr.*, **19** (1965), pp. 210-14.

39. J. D. Bucci, B. K. Robertson, and W. J. James. "Precision Determination of the Lattice Parameters and the Coefficients of Thermal Expansion of $BiFeO_3$," *J. Appl. Crystallogr.*, **5** (1972), pp. 187-91.

40. H. D. Megaw. "The Thermal Expansion of Certain Crystals with Layer Structures," *Proc. Roy. Soc., London,* **A142** (1933), pp. 198-214.

41. H. D. Megaw. "The Thermal Expansion of Crystals in Relation to Their Structure," *Z. Kristallogr.,* **100** (1938), pp. 58-76.

42. V. T. Deshpande and S. V. Suryanarayana. "Thermal Expansion of Cadmium Molybdate," *Curr. Sci.,* **38** (1969), pp. 489-90.

43. K. V. K. Rao, S. V. N. Naidu, and K. S. Murthy. "Precision Lattice Parameters and Thermal Expansion of Calcite," *J. Phys. Chem. Solids,* **29** (1968), pp. 245-48.

44. R. Srinivasan. "The Thermal Expansion of Calcite From Room Temperature up to 400°C," *Proc. Indian Acad. Sci.,* **A42** (1955), pp. 81-85.

45. H. Adenstedt. "Studien Zur Thermischen Ausdehnung Fester Stoffe in Tiefer Temperature (Cu, Ni, Zink Blende, LiF, Kalkspat, Aragonit, NH_4Cl)," *Ann. Phys. (Leipzig),* **26** (1936), pp. 69-96.

46. Liebisch. Physikalische Kristallographie.

47. V. T. Deshpande and S. V. Suryanarayana. "X-Ray Determination of the Thermal Expansion of Calcium Molybdate," *J. Phys. Chem. Solids,* **30** (1969), pp. 2484-86.

48. V. T. Deshpande and S. V. Suryanarayana. "Precision Lattice Parameters and Thermal Expansion of Calcium Tungstate," *J. Mater. Sci.,* **7** (1972), p. 255.

49. K. V. Krishna Rao and S. V. Hagender Naidu. "Thermal Expansion of Stannic Oxide," *J. Osmania Univ. Sci. (India),* **1** (1963), p. 34.

50. H. Fizeau. "Memoire sur la Dilatation des Corps Solides par la Chaleur," *C. R. Acad. Sci. (Paris),* **62** (1866), p. 1133.

51. P. C. Mahanta, J. Hatibarua, and R. K. Das. "Thermal Expansion of Cerium Dioxide by X-Ray Diffraction Method," *J. Sci. Indust. Res.,* **B21** (1962), pp. 596-97.

52. J. Carpkappen, C. W. DeBoon, H. J. M. Lebesque, and B. S. Blaisse. "The Thermal Expansion Coefficients of $La_2Mg_3(NO_3)_{12}\cdot 24H_2O$ and $Ce_2Mg_3(NO_3)_{12}\cdot 24H_2O$ Between 10° and 300°K," *Physica,* **63** (1973), p. 297.

53. K. V. Krishna Rao. "Thermal Expansion of Crystals," in *Physics of the Solid State,* New York, Academic Press, 1969. Pp. 415-26.

54. L. J. Eckert and R. C. Bradt. "Thermal Expaonsion of ^{t}-Ga_2O_3," *J. Amer. Ceram. Soc.,* **56** (1973), p. 229.

55. Z. I. Ezhkova, G. S. Zhdanov, and M. M. Umanskii. "Thermal Expansion Coefficients for GASH, $C(NH_2)_3Al(H_2O)_6(SO_4)_2$," *Kristallografiya,* **3** (1958), pp. 231-32.

56. A. T. Gorton, G. Bitsianes, and T. L. Joseph. "Thermal Expansion Coefficients for Fe and Its Oxide," *Trans. Metall. Soc. AIME (USA),* **233** (1965), pp. 1519-25.

57. S. S. Sharma. "Thermal Expansion of Crystals: Part V. Haematite," *Proc. Indian Acad. Sci.,* **A32** (1950), pp. 285-91.

58. S. V. Suryanarayana and V. T. Deshpande. "X-Ray Determination of the Thermal Expansion of Lead Molybdate," *Curr. Sci.,* **41** (1972), pp. 837-39.

59. V. T. Deshpande and S. V. Suryanarayana. "Lattice Thermal Expansion of Lead Tungstate," *Curr. Sci.,* **40** (1971), pp. 487-89.

60. V. Tscherry, H. Schulz, and M. Czank. "Thermal Expansion of the Lattice Constants of $_{h}$-Eucryptite Single Crystals," *Ber. Deut. Keram. Ges.,* **49** (1972), pp. 153-54.

61. H. D. Megaw. "The Thermal Expansion of Interatomic Bonds, Illustrated by Experimental Evidence From Certain Niobates," *Acta Crystallogr.,* **A24** (1968), pp. 589-604.

62. Y. S. Kim and R. T. Smith. "Thermal Expansion of Lithium Tantalate and Lithium Niobate Single Crystals," *J. Appl. Phys.,* **40** (1969), pp. 4637-41.

63. R. C. Bradt and J. S. Wiley. "Directional Thermal Expansion Coefficients of $_{h}$-MnO_2, *J. Electrochem. Soc.,* **109** (1962), pp. 651.

64. V. T. Deshpande and A. A. Khan. "X-Ray Determination of the Thermal Expansion of Potassium Dihydrogen Arsenate," *Acta Crystallogr.,* **18** (1965), pp. 977-78.

65. A. R. Ubbelohde and I. Woodward. "Structure and Thermal Properties Associated with Some Hydrogen Bonds in Crystals: VII. Behavior of KH_2PO_4 and KH_2AsO_4 on Cooling," *Proc. Roy. Soc. London,* **A188** (1947), pp. 358-71.

66. V. T. Deshpande, R. Pawar, and S. V. Suryanarayana. "Thermal Expansion of Potassium Metaperiodate (KIO_4)," *Curr. Sci.,* **36** (1967), pp. 513-14.

67. L. J. Eckert and R. C. Bradt. "Thermal Expansion of Corundum Structure Rh_2O_3," *Mater. Res. Bull.*, **8** (1973) p. 375.

68. V. T. Deshpande and A. A. Khan. "Thermal Expansion of Rubidium Dihydrogen Phosphate," *Nature (London)*, **209** (1966), p. 608.

69. K. V. Krishna Rao and Murthy K. Satyanarayana. "Thermal Expansion of Scandium Borate," *Indian J. Pure Appl. Phys.*, **11** (1973), pp. 230-31.

70. R. H. Hopkins, J. Deklerk, P. Piotrowski, N. S. Walker, and M. P. Mathur. "Thermal and Elastic Properties of Silicate Oxy-apatite Crystals," *J. Appl. Phys.*, **44** (1973), p. 2456.

71. N. G. Sherstyukov and I. I. Lifanov. "Thermal Expansion of Quartz Single Crystals," *Sov. Phys.-Crystallogr.*, **19** (1975), pp. 681-82.

72. A. N. Amatuni and E. B. Shevchenko. "Linear Thermal Expansion of Quartz and Aluminum Oxide Single Crystals," *Izmer. Tekh.*, No. 10 (1966), pp. 17-20.

73. A. H. Jay. "The Thermal Expansion of Quartz by X-Ray Measurements," *Proc. Roy. Soc. London,* **A142** (1933), p. 237.

74. A. Muller. "Ausdehnungsmessungen auf Gold und auf Kristallinier- tem Quartz zwischen 18° und 520° nach der methode von Fizeau," *Phys. Zeit. (Leipzig)*, **17** (1916), pp. 29-30.

75. Landolt-Börnstein Tables (Springer-Verlag, 1969, Berlin).

76. R. M. Buffington and W. M. Latimer. "The Measurement of Coefficient of Expansion at Low Tempertures: Some Thermodynamic Applications of Expansion Data," *J. Amer. Chem. Soc.*, **48** (1926), p. 2305.

77. K. V. Krishna Rao, S. V. Nagender Naidu, and Leela Iyengar. "Thermal Expansion of Rutile and Anatase," *J. Amer. Ceram. Soc.*, **53** (1970), pp. 124-26.

78. A. Schrauf. "Ueber-die Trimorphie und die Ausdehnungscoefficienten von Titandioxyd," *Kristallogr. Miner. (Liepzig)*, **9** (1884), pp. 433-35.

79. H. Fizeau. "Memoire sur la Dilatation des Corps Solides par la Chaleur," *Acad. Sci., (Paris)*, **62** (1866), p. 62.

80. E. C. Subbarao and K. V. G. K. Gokhale. "Thermal Expansion of Zircon," *Jap. J. Appl. Phys.*, **7** (1968), p. 1126.

81. J. L. Amoros, M. Gutierrez, and M. L. Canut. "La Dilatacion Termica del Nitro NO_3K (sal de Piedra)," *Bol. R. Soc. Espan. Hist. Nat. (Geol.)*, **62** (1964), pp. 23-39.

82. M. A. Lonappan. "Thermal Expansion of Potassium Nitrate," *Proc. Indian Acad. Sci.*, **A41** (1955), p. 239.

83. Benoit. *Travaux et Memoires du Bureau Internacionale des Poids et Mesures 6 (Paris)*.

84. T. Takamori. "Thermal Expansion Characteristics of Polycrystalline Tungsten Oxides," *J. Amer. Ceram. Soc.*, **47** (1964), pp. 534-35.

85. Marc Foex. "Dilatometric Study of the Polymorphism in Mo and W Trioxides," *C. R. Acad. Sci. (Paris)*, **220** (1945), pp. 917-18.

86. C. Rosen, E. Banks, and B. Post. "The Thermal Expansion and Phase Transitions of WO_3," *Acta Crystallogr.*, **9** (1956), pp. 47506.

87. A. K. Sreedhar and R. S. Krishnan. "Thermal Expansion of Muscovite Mica," *J. Indian Inst. Sci.*, **36** (1954), p. 51.

88. S. K. Filatov, V. S. Frank, and Kamenetskii. "Anomalous Thermal Expansion of ZrO_2 and HfO_2 Over the Range 20-1200°C," *Sov. Phy.-Cryst.*, **14** (1970) pp. 696-99.

89. A. K. Sreedhar. "Thermal Expansion of Copper Sulphate ($CuSO_4.5H_2O$)," *J. Indian Inst. Sci.*, **35** (1953), pp. 17-24.

90. G. K. White and J. A. Birch. "Thermal Properties of Silica at Low Temperatures," *Phys. Chem. Glasses*, **6** (1965), pp. 85-89.

91. G. K. White. "Thermal Expansion at Low Temperatures," *Nature (London)*, **187** (1960), pp. 927-29.

92. Robert M. Hazen and Larry W. Finger. *Comparative Crystal Chemistry. Temperature, Pressure, Composition and the Variation of Crystal Structure*. New York, John Wiley & Sons, 1982. 231 pp.

93. A. B. Bobrovskii, G. N. Kartmazov, and V. A. Finkel. "Crystal Structure of Nickel Monoxide at High Temperature," *Izv. Akad. Nauk SSR Neorg. Mater.*, **9** (1973), pp. 1075-76.

94. J. B. Austin. "Thermal Expansion of Some Refractory Oxides," *J. Am. Ceram. Soc.*, **14** (1931), pp. 795-810.

95. B. J. Skinner. "The Thermal Expansions of Thoria, Periclase and Diamond," *Am. Mineral.*, **42** (1957), pp. 39-55.

96. R. J. Beals and R. L. Cook. "Directional Dilatation of Crystal Lattices at Elevated Temperatures," *J. Am. Ceram. Soc.*, **40** (1957), pp. 279-84.

97. I. Suzuki. "Thermal Expansion of Periclase and Olivine, and their Anharmonic Properties," *J. Phys. Earth*, **23** (1975), pp. 145-59.

98. R. M. Hazen. "Effects of Temperature and Pressure on the Cell Dimension and X-Ray Temperature Factors of Periclase," *Am. Mineral.*, **61** (1976a), pp. 266-71.

99. R. E. Carter. "Thermal Expansion of $MgFe_2O_4$, FeO, and MgO_v2/FeO," *J. Am. Ceram. Soc.*, **42** (1959), pp. 324-27.

100. G. R. Rigby, G. H. B. Lovell, and A. T. Green. "Reversible Thermal Expansion and Other Properties of Some Magnesian Ferrous Silicates," *Trans. British Ceram. Soc.*, **45** (1946), pp. 237-50.

101. N. I. Min'ko. "Change in Interion Distances in Oxides in the 298°-1773°K Range," *Zh. Fiz. Khim.*, **46** (1972), pp. 312-15.

102. D. Brooksbank and K. W. Andrews. "Thermal Expansion of Some Inclusions Found in Steels and Relation to Tessellated Streses," *J. Iron and Steel Inst.*, June 1968, pp. 595-99.

103. K. S. Valeev and V. B. Kvaskov. "Thermal Expansion of Bismuth, Cadmium and Zinc Oxides," *Izv. Akad. Nauk. SSSR, Neorg. Mater.*, **9** (1973), pp. 714-15.

104. H. P. Singh and B. Dayal. "Lattice Parameters of Cadmium Oxide at Elevated Temperatures," *Solid State Commun.*, **7** (1969), pp. 725-26.

105. C. F. Grain and W. J. Campbell. "Thermal Expansion and Phase Inversions of Six Refractory Oxides," *U.S. Bureau Mines Rept. Investigation 5982*, 1962, pp. 21.

106. A. J. Eisenstein. "A Study of Oxide Cathods by X-Ray Diffraction Methods," *J. Appl. Phys.*, **17** (1946), pp. 434-43.

107. R. J. Zollweg. "X-Ray Lattice Constant of Barium Oxide," *Phys. Rev.*, **100** (1955), pp. 671-73.

108. V. A. Petukhov. "Single Crystal Aluminum Oxide as a Standard Substance in Dilatometry," *Teplofiz. Vys. Temp.*, **11** (1973), pp. 1083-87.

109. C. P. Kempter and R. O. Elliott. "Thermal Expansion of UN, UO_2, $UO_{2v}ThO_2$, and ThO_2," *J. Chem. Phys.*, **30** (1959), pp. 1524-26.

110. S. Stecura and W. J. Campbell. "Thermal Expansion and Phase Inversion of Rare-Earth Oxides," *U.S. Bureau Mines Rept. Investigation 5847,"* 1962, pp. 47.

111. R. J. Ackermann and C. A. Sorrell. "Thermal Expansion and the High-Low Transformation in Quartz. I. High-Temperature X-Ray Studies," *J. Appl. Cryst.,* **7** (1974), pp. 461-67.

112. T.-S. Chang and P. Trucano. "Lattice Parameter and Thermal Expansion of ReO$_3$ Between 291 and 464 K," *J. Appl. Cryst.,* **11** (1978), pp. 286-288.

113. B. J. Skinner. "Thermal Expansion," in *Handbook of Physical Constants,* ed. by S. P. Clark. *Geological Soc. Am. Memoir,* **97** (1966), pp. 78-96.

114. P. D. Pathak and N. G. Vasavada. "Thermal Expansion of NaCl, KCl, and CsBr by X-Ray Diffraction and the Law of Corresponding States," *Acta Crystallogr.,* **A26** (1970), pp. 655-58.

115. P. D. Pathak, J. M. Trivedi, and N. G. Vasavada. "Thermal Expansion of NaF, KBr, and RbBr and Temperature Variation of the Frequency Spectrum of NaF," *Acta Crystallogr.,* **A29** (1973), pp. 477-79.

116. S. Kumar. "Thermal Expansion of Simple Ionic Crystals," *Proc. Natl. Inst. Sci. India,* **A25** (1959), pp. 364-72.

117. A. L. Larionov and B. Z. Malkin. "Thermal Expansion of Calcium Fluoride," *Phys. Stat. Sol.,* **B60** (1975), pp. K103-K105.

118. B. J. Skinner. "Thermal Expansion of Ten Minerals," *U.S. Geological Survey Professional Paper,* **450D** (1962), pp. 109-12.

119. B. Houston, R. E. Strakna, and H. S. Belson. "Elastic Constants, Thermal Expansion, and Debye Temperature of Lead Telluride," *J. Appl. Phys.,* **39** (1968), pp. 3913-16.

120. M. Ettenberg and R. J. Paff. "Thermal Expansion of AlAs," *J. Appl. Phys.,* **41** (1970), pp. 3926-27.

121. R. Feder and T. Light. "Precision Thermal Expansion Measurements of Semi-Insulating GaAs," *J. Appl. Phys.,* **39** (1968), pp. 4870-1.

122. R. S. Pease. "X-Ray Study of Boron Nitride," *Acta Crystallogr.,"* **5** (1952), pp. 356-61.

123. C. P. Kempter and R. O. Elliott. "Thermal Expansion of UN, UO$_2$, UO$_2$·ThO$_2$, and ThO$_2$," *J. Chem. Phys.,* **30** (1959), pp. 1524-26.

124. W. R. Robinson. "High-Temperature Crystal Chemistry of V_2O_3 and 1 per cent Chromium-Doped V_2O_3," *Acta Crystallogr.*, **B31** (1975), pp. 1153-60.

125. C. E. Rice and W. R. Robinson. "High-Temperature Crystal Chemistry of Ti_2O_3: Structural Changes Accompanying the Semiconductor-Metal Transition," *Acta Crystallogr.*, **B33** (1977), pp. 1342-48.

126. D. R. Peacor. "High-Temperture Single-Crystal X-Ray Study of Natrolite," *Am. Mineral.*, **58** (1973), pp. 676-80.

127. E. P. Meagher and G. A. Lager. "Polyhedral Thermal Expansion in the TiO_2 Polymorphs: Refinement of the Crystal Structures of Rutile and Brookite at High Temperature," *Canadian Mineral.*, **17** (1979), pp. 77-85.

128. M. Horn, C. F. Schwerdtfeger, and E. P. Meagher. "Refinement of the Structure of Anatase at Several Temperatures," *Z. Kristallogr.*, **136** (1972), pp. 3913-16.

129. E. P. Meagher. "The Crystal Structures of Pyrope and Grossularite at Elevated Temperatures," *Am. Mineral.*, **60** (1975), pp. 218-28.

130. R. M. Hazen. "Effects of Temperature and Pressure on the Crystal Structure of Forsterite," *Am. Mineral.*, **61** (1976b), pp. 1280-93.

131. G. E. Brown and C. T. Prewitt. "High-Temperture Crystal Chemistry of Hortonolite," *Am. Mineral.*, **58** (1973), pp. 577-87.

132. J. R. Smyth and R. M. Hazen. "The Crystal Structures of Forsterite and Hortonolite at Several Temperatures up to 900°C," *Am. Mineral.*, **58** (1973), pp. 588-593.

133. J. R. Smyth. "High Temperature Crystal Chemistry of Fayalite," *Am. Mineral.*, **60** (1975), pp. 1092-97.

134. L. W. Finger, R. M. Hazen, Y. Yagi. "Crystal Structures and Electron Densities of Nickel and Iron Silicate Spinels at Elevated Temperature or Pressure," *Am. Mineral.*, **64** (1979), pp. 1002-9.

135. M. Taylor and G. E. Brown. "High-Temperature Structural Study of the $P2_1/a$-$A2/a$ Phase Transition in Synthetic Titanite, $CaTiSiO_5$," *Am. Mineral.*, **61** (1976) pp. 435-47.

136. B. A. Wechsler. "Cation Distribution and High-Temperature Crystal Chemistry of Armalcolite," *Am. Mineral.*, **62** (1977), pp. 913-20.

137. A. M. Glazer and S. A. Mabud. "Powder Profile Refinement of Lead Zirconate Titanate at Several Temperatures. II. Pure $PbTiO_3$," *Acta Crystallogr.*, **B34** (1978), pp. 1065-70.

138. S. Sueno, M. Cameron, and C. T. Prewitt. "Orthoferrosilite: High Temperature Crystal Chemistry," *Am. Mineral.*, **61** (1976), pp. 38-53.

139. J. R. Smyth. "An Orthopyroxene Structure up to 850°C," *Am. Mineral.*, **58** (1973), pp. 636-848.

140. J. R. Smyth. "The High-Temperature Crystal Chemistry of Clinohypersthene," *Am. Mineral.*, **59** (1974), pp. 1069-82.

141. M. Cameron, S. Sueno, C. T. Prewitt, and J. J. Papike. "High-Temperature Crystal Chemistry of Acmite, Diopside, Hedenbergite, Jadeite, Spodumene, and Ureyite," *Am. Mineral.*, **58** (1973), pp. 594-618.

142. C. T. Prewitt, S. Sueno, and J. J. Papike. "The Crystal Structures of High Albite and Monalbite at High Temperatures," *Am. Mineral.*, **61** (1976), pp. 1213-25.

143. J. K. Winter, F. P. Okamura, and S. Ghose. "A High-Temperature Structural Study of High Albite, Monalbite, and the Analbite-Monalbite Phase Transition," *Am. Mineral.*, **64** (1979), pp. 409-23.

144. J. K. Winter, S. Ghose, and F. P. Okamura. "A High-Temperature Study of the Thermal Expansion and the Anisotropy of the Sodium Atom in Low Albite," *Am. Mineral.*, **62** (1977), pp. 921-31.

145. F. F. Foit and D. R. Peacor. "The Anorthite Crystal Structure at 410 and 830°C," *Am. Mineral.*, **58** (1973), pp. 665-75.

146. N. Foreman and D. R. Peacor. "Refinement of the Nepheline Structure at Several Temperatures," Z. *Kristallogr.*, **132** (1970), pp. 45-70.

147. M. F. Hochella, G. E. Brown, F. K. Ross, and G. V. Giggs. "High-Temperature Crystal Chemistry of Hydrous Mg- and Fe-Cordierites," *Am. Mineral.*, **64** (1979), pp. 337-51.

148. H. Takeda and B. Morosin. "Comparison of Observed and Predicted Structural Parameters of Mica at High Temperature," *Acta Crystallogr.*, **B31** (1975), pp. 2444-52.

149. J. K. Winter and S. Ghose. "Thermal Expansion and High-Temperature Crystal Chemistry of the Al_2SiO_5 Polymorphs," *Am. Mineral.*, **64** (1979), pp. 573-86.

150. W. W. Pillars and D. R. Peacor. "The Crystal Structure of $_b$-Eucryptite as a Function of Temperature," *Am. Mineral.*, **58** (1973), pp. 681-90.

151. S. Sueno, M. Cameron, J. J. Papike, and C. T. Prewitt. "The High Temperature Crystal Chemistry of Tremolite," *Am. Mineral.*, **58** (1973), pp. 649-64.

152. D. E. Cox and A. W. Sleight. "Mixed-Valent $Ba_2Bi^{3+}Bi^{5+}O_6$: Structure and Properties Versus Temperature," *Acta Crystallogr.*, **B35** (1979), pp. 1-10.

153. G. E. Brown, C. T. Prewitt, J. J. Papike, and S. Sueno. "A Comparison of the Structures of Low and High Pigeonite," *J. Geophys. Res.*, **77** (1972), pp. 5778-89.

154. A. S. Koster, J. P. P. Renaud, and G. D. Rieck. "The Crystal Structures at 20 and 1000°C of Bismuth Uranate, Bi_2UO_6," *Acta Crystallogr.*, **B31** (1975), pp. 127-31.

155. J. R. Smyth. "Orthopyroxene-High-Low Clinopyroxene Inversions," *Earth Planet. Sci. Lett.*, **6** (1969), pp. 406-7.

156. J. R. Smyth. "Protoenstatite: A Crystal-Structure Refinement at 1100°C," *Z. Kristallogr.*, **134** (1971), pp. 262-74.

157. J. R. Smyth and C. W. Burnham. "The Crystal Structures of High and Low Clinohypersthene," *Earth Planet. Sci. Lett.*, **14** (1972), pp. 183-89.

158. S. Sueno, J. J. Papike, C. T. Prewitt, and G. E. Brown. "Crystal Structure of Cummingtonite," *J. Geophys. Res.*, **77** (1972) pp. 5767-77.

159. R. E. Hanneman, H. C. Gatos. "The Relation Between Compressibility and Thermal Expansion Coefficients in Cubic Metals and Alloys," *J. Appl. Phys.*, **36** (1965), pp. 1794-96.

160. L. G. Van Uitert, H. M. O'Bryan, H. J. Guggenheim, R. L. Barns, and G. O. Zydzik. "Correlation of the Thermal Expansion Coefficients of Rare Earth and Transition Metal Oxides and Fluorides," *Mater. Res. Bull.*, **12** (1977), pp. 307-314.

161. L. G. Van Uitert, H. M. O'Bryan, H. J. Guggenheim, R. L. Barns, and G. O. Zydzik. "Thermal Expansion--An Empirical Correlation," *Mater. Res. Bull.*, **12** (1977), pp. 261-268.

162. C. E. Holcombe, Jr. "Thermal Expansion Coefficients for Low Expansion Oxices," *High Temp. Sci.*, **12** (1980), pp. 63-66.

163. C. E. Holcombe, Jr. "Thermal Expansion Coefficients for Low Expansion Oxides," *Ceramic Bull.*, **59(12)** (1980), pp. 1219-20.

164. C. E. Holcombe, Jr. "Ternary Tantalate Compositions," *J. Mater. Sci.*, **14(9)** (1979), pp. 2255-60.

165. C. E. Holcombe and D. D. Smith. "Characterization of the Thermally Contracting Tungstates, $Ta_{22}W_4O_{67}$, Ta_2WO_8, and $Ta_{16}W_{18}O_{94}$," *J. Am. Ceram. Soc.*, **61** (1978), pp. 163-69.

166. R. Ruh, G. W. Hollenberg, S. R. Skaggs, S. D. Stoddard, and F. D. Gac. "Axial and Linear Thermal Expansion of ZrO_2 and HfO_2," *Am. Ceram. Soc. Bull.* **60(4)** (1981), pp. 504-506.

167. R. Ruh, G. W. Hollenberg, E. G. Charles, and V. A. Patel. "Phase Relations and Thermal Expansion in the System HfO_2-TiO_2," *J. Am. Ceram. Soc.*, **59** (1976), pp. 495-99.

168. J. J. Cleveland and R. C. Bradt. "Grain Size-Thermal Expansion Anisotropy Effects on Strength and Fracture of Pseudobrookites," *Ceram. Soc. Bull.*, **55** (1976), p. 396.

169. J. E. Blendell, R. L. Cable, and R. J. Charles. in *Ceramic Microstructures: Proceedings of 6th (1976) International Materials Symposium,* Westview Press, Boulder, Colo., 1977 (R. W. Fulrath and J. A. Pask, eds.). Pp. 721-730.

INITIAL DISTRIBUTION

7 Naval Air Systems Command
  AIR-33E, Andrew Glista (5)
  AIR-723 (2)
2 Naval Sea Systems Command (SEA-09B312)
1 Commander in Chief, U. S. Pacific Fleet (Code 325)
1 Commander, Third Fleet, Pearl Harbor
2 Naval Academy, Annapolis (Director of Research)
3 Naval Ship Weapon Systems Engineering Station, Port Hueneme
  Code 5711, Repository (2)
  Code 5712 (1)
1 Naval War College, Newport
1 Air Force Intelligence Service, Bolling Air Force Base (AFIS/INTAW, Maj. R. Lecklider)
12 Defense Technical Information Center
3 Kimble Applied Research & Development, Toledo, OH (T. W. Brock)
5 Litton Systems Inc., Woodland Hills, CA (Frans G. A. DeLaat)
4 Singer Company, Little Falls, NJ (Michael Tarasivich)

END

10-86

DTIC